

**ISTANBUL TECHNICAL UNIVERSITY ★ GRADUATE SCHOOL OF  
SCIENCE ENGINEERING AND TECHNOLOGY**

**MODELING AND INTERPRETING TRANSIENT WELLBORE  
TEMPERATURE BEHAVIORS IN WELLBORES UNDER NONISOTHERMAL  
SINGLE-PHASE LIQUID FLOW CONDITIONS IN OIL RESERVOIRS**



**M.Sc. THESIS**

**Gonca ÜLKER**

**Department of Petroleum and Natural Gas Engineering**

**Petroleum and Natural Gas Engineering Programme**

**JANUARY 2018**



**ISTANBUL TECHNICAL UNIVERSITY ★ GRADUATE SCHOOL OF**  
**SCIENCE ENGINEERING AND TECHNOLOGY**

**MODELING AND INTERPRETING TRANSIENT WELLBORE  
TEMPERATURE BEHAVIORS IN WELLBORES UNDER NONISOTHERMAL  
SINGLE-PHASE LIQUID FLOW CONDITIONS IN OIL RESERVOIRS**

**M.Sc. THESIS**

**Gonca ÜLKER  
(505151502)**

**Department of Petroleum and Natural Gas Engineering**

**Petroleum and Natural Gas Engineering Programme**

**Thesis Advisor: Prof. Dr. Mustafa ONUR**

**JANUARY 2018**



**İSTANBUL TEKNİK ÜNİVERSİTESİ ★ FEN BİLİMLERİ ENSTİTÜSÜ**

**PETROL REZERVUARLARINDA TEK-FAZLI SIVI AKIŞI KOŞULLARINDA  
KUYUİÇİ KARARSIZ SICAKLIK DAVRANIŞLARININ MODELLENMESİ VE  
YORUMLANMASI**

**YÜKSEK LİSANS TEZİ**

**Gonca ÜLKER  
(505151502)**

**Petrol ve Doğal Gaz Mühendisliği Anabilim Dalı**

**Petrol ve Doğal Gaz Mühendisliği Programı**

**Tez Danışmanı: Prof. Dr. Mustafa ONUR**

**OCAK 2018**



Gonca ULKER, an M.Sc. student of ITU Graduate School of Petroleum Engineering student ID 505151502, successfully defended the thesis entitled “MODELING AND INTERPRETING TRANSIENT WELLBORE TEMPERATURE BEHAVIORS IN WELLBORES UNDER NONISOTHERMAL SINGLE-PHASE LIQUID FLOW CONDITIONS IN OIL RESERVOIRS”, which she prepared after fulfilling the requirements specified in the associated legislations, before the jury whose signatures are below.

**Thesis Advisor :**      **Prof. Dr. Mustafa ONUR** .....  
Istanbul Technical University

**Jury Members :**      **Yrd. Doç. Dr. İhsan Murat GÖK** .....  
Istanbul Technical University

**Prof. Dr. İbrahim KOCABAŞ** .....  
Katip Celebi University

**Date of Submission** : 17 Nov 2017  
**Date of Defense** : 04 Jan 2018





*To my family and friends,*



## **FOREWORD**

In this work, main purpose is to investigate the transient wellbore temperature behaviors in wellbores under nonisothermal single-phase liquid flow conditions in oil reservoirs.

I would like to thank my thesis advisor Prof. Dr. Mustafa ONUR for his support on the studies of my thesis. Also, I would like to thank Asst. Prof. Dr. Ihsan Murat GOK for help in learning and improving analytical methods in reservoir engineering.

Finally, I would like to thank my family and my friends for their supports during this work.

December 2017

Gonca ULKER  
(Petroleum Engineer)



## TABLE OF CONTENTS

	<u>Page</u>
<b>FOREWORD</b> .....	<b>ix</b>
<b>TABLE OF CONTENTS</b> .....	<b>xi</b>
<b>SYMBOLS</b> .....	<b>xiii</b>
<b>LIST OF TABLES</b> .....	<b>xv</b>
<b>LIST OF FIGURES</b> .....	<b>xvii</b>
<b>ACKNOWLEDGEMENTS</b> .....	<b>xix</b>
<b>SUMMARY</b> .....	<b>xxi</b>
<b>ÖZET</b> .....	<b>xxiii</b>
<b>1. INTRODUCTION</b> .....	<b>1</b>
1.1 Background and Literature Review.....	1
1.2 Problem Statement .....	2
1.3 Objective of Research .....	2
1.4 Significance of Study .....	3
1.5 Scopes of Study.....	3
1.6 Thesis Structure.....	3
<b>2. WELLBORE MASS AND MOMENTUM FLUID FLOW MODEL EQUATIONS</b> .....	<b>5</b>
2.1 Conventional Wellbore Storage Model.....	5
2.2 Momentum Model.....	11
<b>3. WELLBORE HEAT FLOW MODEL EQUATIONS</b> .....	<b>21</b>
3.1 Derivation of Transient Wellbore Thermal Energy Equation.....	21
3.1.1 Overall heat transfer coefficient.....	23
3.1.2 Correlations for dimensionless heat transfer functions.....	24
3.1.3 Earth geothermal gradient modeling.....	26
3.2 Transient Wellbore Temperature Solutions .....	26
3.2.1 Specified production case-single phase oil systems .....	26
3.2.2 Buildup case for-single phase oil systems .....	31
3.3 Steady-State Wellbore Temperature Solutions .....	38
3.3.1 Specified production case-single phase oil systems .....	38
3.3.2 Buildup case for single-phase oil systems .....	39
<b>4. COUPLING WITH TRANSIENT SANDFACE / BOTTOMHOLE PRESSURE AND TEMPERATURE SOLUTIONS</b> .....	<b>41</b>
4.1 Transient Bottomhole Pressure .....	41
4.2 Transient Wellbore Pressure Distribution Solution .....	43
4.3 Transient Wellbore Flow Rate Distribution Solution.....	44
4.4 Numerical Inversion of Solutions .....	45
<b>5. SANDFACE AND WELLBORE PRESSURE, FLOW RATE AND TEMPERATURE BEHAVIORS</b> .....	<b>47</b>
5.1 Sandface Flow Rate Behavior for Production and Buildup Cases.....	48

5.2 Flow Rate and Pressure Distrubitions along the Wellbore for Production and Buildup Cases .....	49
5.3 Wellbore Temperature Behavior for Production and Buildup Cases .....	56
<b>6. IMPACT OF VARIOUS PARAMETERS ON SANDFACE AND WELLBORE TEMPERATURE .....</b>	<b>59</b>
6.1 Geothermal Gradient at a Fixed Gauge Location for Production and Buildup .....	59
6.2 Effect of Earth Conductivity and Diffusivity at a Fixed Gauge Location in Production and Buildup .....	60
6.3 Effect of Production Flow Rate at a Fixed Gauge Location .....	61
<b>7. ANALYSIS OF INTERPRETATION OF TRANSIENT WELLBORE TEMPERATURES .....</b>	<b>63</b>
<b>8. CONCLUSIONS.....</b>	<b>65</b>
<b>REFERENCES .....</b>	<b>67</b>
<b>CURRICULUM VITAE .....</b>	<b>71</b>



## SYMBOLS

<b>A</b>	: Cross-sectional area of the pipe, m <sup>2</sup>
<b>B</b>	: Formation volume factor, m <sup>3</sup> /sm <sup>3</sup>
<b>c</b>	: Isothermal compressibility, Pa <sup>-1</sup>
<b>C</b>	: Wellbore storage coefficient, m <sup>3</sup> /Pa
<b>c<sub>p</sub></b>	: Specific heat capacity, J/kg-K
<b>D</b>	: Pipe inside diameter, m
<b>f</b>	: Friction factor, unitless
<b>h</b>	: Reservoir thickness, m
<b>H</b>	: Specific enthalpy, J/kg
<b>k</b>	: Effective permeability, m <sup>2</sup>
<b>L</b>	: Wellbore Length, m
<b>m</b>	: Mass of fluid per unit depth, kg/m
<b>m<sup>l</sup></b>	: Mass of wellbore system per unit depth, kg/m
<b>N<sub>stef</sub></b>	: Stehfest Parameter, unitless
<b>p</b>	: Pressure, Pa
<b>q</b>	: Volumetric flow rate at standard conditions, sm <sup>3</sup> /s
<b>r</b>	: Radius, m
<b>R<sub>e</sub></b>	: Reynolds number, unitless
<b>S</b>	: Skin factor, unitless
<b>t</b>	: Time, s
<b>T</b>	: Temperature, K
<b>U<sub>t</sub></b>	: Overall heat transfer coefficient, J/s.m <sup>2</sup> .K
<b>v</b>	: Vector of velocity, m/s
<b>s</b>	: Laplace variable
<b>w</b>	: Mass rate, kg/s
<b>z</b>	: Gauge location from top of the formation, m
<b>α</b>	: Thermal diffusivity constant, m <sup>2</sup> /s
<b>β</b>	: Thermal expansion coefficient, K <sup>-1</sup>
<b>ε<sub>JT</sub></b>	: Joule-Thomson expansion coefficient, K/Pa
<b>φ</b>	: Porosity, fraction
<b>λ</b>	: Thermal conductivity, J/m-s-K
<b>μ</b>	: Viscosity of fluid, Pa.s
<b>ρ</b>	: Density, kg/m <sup>3</sup>
<b>ω</b>	: Acentric factor, unitless
<b>δ</b>	: Pipe roughness, m
<b>Ψ</b>	: Unit-impulse response

### Superscripts

<b>w</b>	: Wellbore
<b>0</b>	: Initial conditions

### Subscript

<b>bh</b>	: Bottomhole
-----------	--------------

**e** : Outer radius  
**f** : Fluid  
**o** : Oil  
**p** : Constant pressure or isobaric  
**s** : Solid  
**sf** : Sandface  
**t** : Total  
**T** : Temperature  
**wh** : Well head



## LIST OF TABLES

	<u>Page</u>
<b>Table 3.1</b> : Comparison of Approximate and Rigorous $T_D$ Solutions .....	<b>25</b>
<b>Table 4.1</b> : Well, Wellbore and Earth Physical and Thermal Property Input Data...	<b>45</b>
<b>Table 5.1</b> : Simulation Input Data Used for Verification Example (Onur and Cinar 2016). .....	<b>47</b>
<b>Table 5.2:</b> Skin Zone Parameters for Verification Example (Onur and Cinar 2016).	<b>47</b>



## LIST OF FIGURES

	<u>Page</u>
<b>Figure 2.1</b> : A cylindrical homogeneous reservoir with a vertical well where the well head flow is controlled, and the bottomhole flow rate pressure and temperature are measured..	5
<b>Figure 4.1</b> : Effect of skin-zone properties on sandface flow rates computed from the WBS model for drawdown..	46
<b>Figure 4.2</b> : Effect of skin-zone properties on sandface flow rates computed from the momentum model for drawdown.	46
<b>Figure 5.1</b> : Comparison of sandface flow rates inverted by the Stehfest and Crump algorithms for the WBS and momentum models for drawdown; skin zero case..	48
<b>Figure 5.2</b> : Comparison of sandface flow rates inverted by the Stehfest and Crump algorithms for the WBS and momentum models for buildup; skin zero case..	49
<b>Figure 5.3</b> : $z$ vs $p^w$ plot at various drawdown times, momentum model, zero skin case..	50
<b>Figure 5.4</b> : $z$ vs $dp^w/dz$ plot at various drawdown times, momentum model, zero skin case	51
<b>Figure 5.5</b> : $z$ vs $q^w$ plot at various drawdown times, momentum model, zero skin case..	52
<b>Figure 5.6</b> : $z$ vs $dq^w/dz$ plot at various drawdown times, momentum model, zero skin case..	53
<b>Figure 5.7</b> : $z$ vs $dp^w/dz$ plot at various buildup elapsed times, momentum model, zero skin case..	54
<b>Figure 5.8</b> : $z$ vs $abs(dq^w/dz)$ plot at various buildup elapsed times, momentum model, zero skin case..	55
<b>Figure 5.9</b> : Effect of skin on $q^w$ along the wellbore at various drawdown elapsed times, momentum model..	56
<b>Figure 5.10</b> : Effect of gauge location inside the wellbore on transient temperatures during drawdown; zero skin case..	57
<b>Figure 5.11</b> : Effect of gauge location inside the wellbore on transient temperatures during buildup; zero skin case..	57
<b>Figure 5.12</b> : $z$ vs $T^w$ plot at various drawdown times, momentum model, zero skin case..	58
<b>Figure 5.13</b> : $z$ vs $T^w$ plot at various buildup times, momentum model, zero skin case..	58
<b>Figure 6.1</b> : Effect of Earth Geothermal Gradient for $z=500$ m..	59
<b>Figure 6.2</b> : Effect of Earth Conductivity for $z=500$ m..	60
<b>Figure 6.3</b> : Effect of Earth Diffusivity for $z=500$ m..	61
<b>Figure 6.4</b> : Effect of Production Flow Rate for $z=0$ m..	62
<b>Figure 6.5</b> : Effect of Production Flow Rate for $z=100$ m..	62

**Figure 7.1** : Comparison of sandface and wellbore drawdown temperature-derivatives with skin and momentum effects at different gauge locations (Onur et al.,2016)..... **63**

**Figure 7.2** : Comparison of sandface and wellbore buildup temperature-derivatives with skin and momentum effects at different gauge locations (Onur et al.,2016)..... **64**



## **ACKNOWLEDGEMENTS**

Some of the results and graphs of this MS thesis have been presented in SPE Paper 181710 and published in SPE Journal in 2017.





**MODELING AND INTERPRETING TRANSIENT WELLBORE  
TEMPERATURE BEHAVIORS IN WELLBORES UNDER  
NONISOTHERMAL SINGLE-PHASE LIQUID FLOW CONDITIONS IN OIL  
RESERVOIRS**

**SUMMARY**

Currently, the transient temperature data can be useful to predict reservoir and wellbore parameters. With developing technology, temperature sensors can recognize small temperature changes like 0.01 K or less; thus, researchers use transient temperature data for parameter estimation in reservoir or wellbore. Near wellbore zone, parameter estimation from the transient pressure data is difficult because the pressure changes hastily near wellbore zone. Generally, it is assumed that fluid flow is isothermal in the reservoir although it is nonisothermal. There are some factors which cause thermal changes in reservoir as J-T coefficient, adiabatic expansion or compression, convection and conduction. So, the heat flow model should be used to model and interpret wellbore temperature data.

In this work, the transient wellbore temperature distributions in wellbores are modeled and interpreted under nonisothermal single-phase liquid flow conditions for oil reservoirs. By using mass, momentum and energy balance equations, the temperature behaviors are obtained for transient and steady state conditions in drawdown and buildup periods. Then, the analytical solutions are coupled with sandface pressure and temperature solutions derived by Kocak (2017) in Laplace space.

Derived equations in the solution of analytical model are conventional wellbore storage (WBS) model equation by using mass balance, momentum equation, and heat flow model equation. These equations provide transient and steady state wellbore temperature distributions in drawdown and buildup. With these distributions, the effects of various parameters on sandface and wellbore temperature can be investigated. Also, the parameters such as permeability, skin, J-T coefficient, earth

thermal conductivity can be estimated from transient wellbore temperatures along with transient wellbore pressure data.

All of equations derived in this work provide transient temperature data for single phase and slightly compressible fluid for a vertical wellbore in drawdown and buildup periods, for nonisothermal conditions. These data can be used to estimate reservoir and fluid properties, but drawdown temperature data is more crucial due to exhibiting discernable flow regimes. Also, we can not see any distinguishable flow regimes in buildup temperature behaviors.



**PETROL REZERVUARLARINDA TEK-FAZLI SIVI AKIŞI  
KOŞULLARINDA KUYUIÇİ KARARSIZ SICAKLIK DAVRANIŞLARININ  
MODELLENMESİ VE YORUMLANMASI**

**ÖZET**

Günümüzde, kararsız sıcaklık verilerinin kullanımı kuyuiçi ve rezervuar parametrelerinin belirlenmesinde önemli bir yer almıştır. Sıcaklık verilerini belirlemek için hassas ölçümler yapan aletlerin geliştirilmesi kararsız sıcaklık analizleri için önemli bir gelişme olmuştur. Kuyuiçi civarı parametrelerin tahmininde kararsız basınç analizinin yetersiz kaldığı görülmüştür. Bu sebeple, kirlenme zonu faktörü ve kirlenme zonu yarı çapı gibi parametrelerin belirlenmesinde araştırmacılar kararsız sıcaklık analizini kullanmaya başlamıştır. Rezervuardaki akış izotermal değildir ve rezervuarda sıcaklık değişimine sebep olan bazı önemli ısı transferi mekanizmaları vardır: Joule-Thomson etkisi, ısı iletimi ve yayılımı, adyabatik genişleme/sıkışma. Sıcaklık verilerini modellerken bu ısı transfer mekanizmaları kullanılmaktadır.

Bu çalışmada, petrol rezervuarları için izotermal olmayan tek fazlı sıvı akış koşullarındaki kararsız kuyuiçi sıcaklık davranışları incelenmiştir. Kararsız ve kararlı akış koşullarında sıcaklık dağılımları elde edilirken kütle, momentum ve enerji denklemleri kullanılmıştır. Elde edilen analitik modeller Kocak (2017) tarafından Laplace uzayında çözülen kuyudibi basınç ve sıcaklık çözümleri ile birleştirilmiştir.

Isı transferi mekanizmaları kullanılarak analitik olarak türetilen denklemler şunlardır: Konvensiyonel kuyuiçi depolama denklemi, momentum denklemi, ısı transferi denklemi. Bu denklemler ile üretim ve üretim kapama dönemleri için kararlı ve kararsız kuyuiçi sıcaklık dağılımları elde edilir. Elde edilen sıcaklık dağılımları rezervuar ve kuyuiçi parametrelerinin kuyudibi ve kuyuiçi sıcaklık değişimleri üzerindeki etkilerinin görülmesini sağlar. Dahası, kirlenme zonu faktörü, geçirimsizlik, J-T katsayısı, ısı iletkenlik gibi parametreler tahmin edilebilir.

Çalışmada ilk olarak kütle korunum denklemi kullanılarak konvensiyonel kuyuiçi depolama modeli elde edilir. Bu model elde edilirken, 1 boyutlu ve tek fazlı petrol akışının olduğu, rezervuar ve ısı parametrelerinin sıcaklık ve basınç ile değişmediği, kuyunun rezervuara dik olduğu ve yerçekimi etkilerinin ihmal edildiği kabul edilir. Ayrıca, model türetilirken izotermal sıkıştırılabilirlik ve izobaric ısı genişleme katsayılarının tanımları kullanılır. Kuyu kesit alanının sabit olduğu kabul edilir. Kütle korunumu modelinde momentum korunumu ihmal edilir. Daha sonra, basınç kuvvetlerini, sürtünme kayıplarını ve yerçekimi etkilerini içeren momentum denklemi yazılarak momentum modeli elde edilir. Sürtünme kayıplarını elde etmek için Darcy-Weishbach sürtünme denklemi kullanılır. Bu denklemde önemli olan ters akışa izin vermek için hızın karesini yazarken mutlak değer kullanmaktır. Kütle ve

momentum korunumu denklemleri elde edilirken Mansori (2015) nin yaklaşımı takip edilir. İç ve dış sınır koşulları kullanılarak Laplace uzayında elde edilen denklemlerle basınç ve akış hızı profilleri elde edilir.

Kullanılması gereken diğer önemli model kararsız kuyuiçi ısı enerji denkleminin türetilmesidir. Bu modelin türetilmesi Hasan ve Kabir (2005) tarafından verilir. Ancak buradaki tek fark, onların çalışmasında kullanılan derinlik koordinatı  $z$ , kuyubaşından kuyudibi yönüne doğru pozitif iken bu çalışmada kuyudibinden kuyubaşı yönüne doğru pozitifdir. Isıl enerji denkleminin türetilmesinin başlangıç noktası enerji korunumu denkleminin yazılmasıdır. Enerji korunumu denklemi bazı önemli parametreleri içerir: Entalpi, kütle hızı, derinlik. Formasyondan alınan veya formasyona verilen ısı tanımından yararlanılarak kuyuiçi ısı akış modeli oluşturulmaya çalışılır. Ayrıca, Sagar (1991) tarafından türetilen ısı transferi katsayısı denklemi ve Hasan ve Kabir (1994) tarafından türetilen boyutsuz ısı transfer fonksiyonu kullanılır. Çalışmanın tümünde jeotermal gradyan 0.03 K/m olarak kullanılır.

Bu ısı transfer mekanizmaları ile üretim ve üretim kapama dönemleri için öncelikle kararsız kuyuiçi sıcaklık sonuçlarına ulaşılır. Daha sonra kararlı kuyuiçi sıcaklık sonuçlarına ulaşmak için kararsız kuyuiçi sıcaklık denklemlerinde zamanın sonsuza gittiği varsayımı yapılır. Aynı varsayım üretim kapama dönemi için üretim kapama zamanının sonsuza gitmesi olarak ele alınır.

Kocak (2017) tarafından elde edilen kararsız kuyuiçi ve kuyudibi basınç ve akış hızı denklemleri ile çalışmada elde edilen kararsız kuyuiçi sıcaklık denklemleri birleştirilir. Çözümlerin sayısal çevriminde iki önemli algoritma kullanılır: Stehfest (1970) ve Crump (1976) algoritmaları. Crump algoritmasının momentum çözümleri için daha uygun olduğu grafiksel olarak gösterilir ve bu algoritma çalışmadaki bütün modellerin elde edilmesinde kullanılır.

Elde edilen kararsız kuyuiçi sıcaklık denklemleri Onur ve Cinar (2016) ın kullanmış olduğu parametrelerle değerlendirilir ve grafiklerle görselleştirilir. Öncelikle kuyuiçi basınç parametresinin kuyuiçi derinlik koordinatı  $z$  ile değişim grafiği elde edilir. Aynı grafik kütle hızı parametresi için de elde edilir. Tüm bu grafikler farklı kirlenme zonu parametreleri için de değerlendirilir ve negatif kirlenme zonu parametresinin kuyuiçi akış hızını artırdığı, pozitif kirlenme zonu parametresinin ise kuyuiçi akış hızını azalttığı gözlemlenir.

Kirlenme zonu parametresinin sıfır olduğu kabul edilen durumda, kuyudibinden kuyubaşına doğru gidildikçe kuyuiçi sıcaklığının formasyona verilen ısı sebebiyle azaldığı gözlemlenmiştir. Formasyona verilen ısının sebebi ölçü aletinin bulunduğu derinlikte formasyonun daha düşük sıcaklığa sahip olmasıdır. Üretim döneminin geç zamanlarında ölçüm noktasındaki kuyuiçi sıcaklığı kuyuiçine giren sıvının sıcaklığının artmasıyla artar. Fakat, sabit ölçüm noktası için üretim kapama döneminin geç zamanlarındaki kuyuiçi sıcaklığı sabit yüzey sıcaklığına yaklaşır.

Elde edilen kuyuiçi sıcaklık dağılımlarının çeşitli parametrelerle değişimi incelenir. Bu incelemelerde farklı kirlenme zonu parametreleri kullanılır. Sabit ölçüm noktası derinliğinde, üretim ve üretim kapama dönemlerinde negatif ve pozitif kirlenme zonu değerleri için jeotermal gradyan arttıkça kuyuiçi sıcaklığının azaldığı gözlemlenir. Isıl iletkenliğin sadece üretim döneminde minimum düzeyde etkisi olduğu üretim kapama döneminde ise etkisinin olmadığı gözlemlenir. Artan ısı iletkenliğin kuyuiçinde sıcaklığı düşürdüğü gözlemlenir. Diğer bir inceleme üretim akış hızının kuyuiçi sıcaklığı üzerindeki etkisini gözlemlenmek için yapılır. Akış hızının

artmasıyla kuyuiçi sıcaklığının arttığı görülür. Ancak bu sıcaklık artışı ölçüm noktasının kuyudibinden uzaklaşmasıyla daha net anlaşılır.

Çalışmanın tamamından elde edilen kuyuiçi sıcaklık ve türevinin zamanla değişim grafiği sonuçların yorumlanmasında kullanılır. Üretim dönemi için elde edilen grafiklerden akış rejimlerinin belirlenebildiği ve bu akış rejimleri sonucunda kirlenme zonu ve bu zonu dışında kalan bölge için rezervuar parametrelerinin belirlenebildiği gözlemlenir. Ancak, üretim kapama dönemi için elde edilen sıcaklık grafiklerinden akış rejimlerinin belirlenemediği anlaşılır.

Bu çalışmada türetilen bütün denklemler izotermal olmayan koşullarda tek fazlı sıvı akışı için kararsız sıcaklık verisi sağlar. Bu veriler rezervuar parametrelerini belirlemek için kullanılabilir, fakat üretim dönemi sıcaklık verisi akış rejimlerini belirlemek için kullanıldığından daha önemlidir.





## 1. INTRODUCTION

### 1.1 Background and Literature Review

Recent studies show that like pressure data, transient temperature data can be used to estimate the rock and fluid parameters. One of the main reasons that motivates the use of temperature transient data is due to new upgrades in temperature-measurement devices temperatures can now be measured with a resolution better than 0.01 K (Duru and Horne 2011a; Al-Nahdi et al. 2014; Sidorova et al. 2015).

The studies in the petroleum and geothermal engineering display impressive heating and cooling behaviours of sandface temperatures during constant rate drawdown and buildup tests if there are the impacts of Joule-Thomson heating/cooling, transient-adiabatic-fluid expansion/compression, conduction, and convection in the modeling. Generally, temperature changes during fluid production are small compared with to pressure changes; however, some temperature changes in the high-pressure-drawdown conditions become more conspicuous. With the nonlinear-regression and sensitivity analysis, it has been displayed that information regarding petrophysical properties such as porosity and permeability could be inferred from the temperature-transient data (Onur and Cinar, 2016).

The first classical study about analytical temperature equation for estimating steady state wellbore temperature distribution along the wellbore was presented by Ramey (1962). This work was for a vertical wellbore of an injection well under nonisothermal flow. The Ramey (1973) analytical steady-state wellbore-temperature equation was modified by Curtis and Witterholt for producing wells. Later, Alves et al. and Hasan and Kabir have presented steady-state analytical equation for estimating wellbore temperature changes in 1992 and 1994, respectively.

In the literature, "Hasan, Kabir and Lin" (1990) were the first to present an analytical wellbore-temperature equation. Their study was to predict transient wellbore temperature along the wellbore for drawdown and buildup tests under single-phase fluid flow in the wellbore. After Hasan et al., "Izgec, Kabir, Zhu and Hasan"s (2007)

transient fluid and heat flow modelling, App's (2010) nonisothermal and productivity behavior of high pressure reservoirs, and "Duru and Horne's (2010) reservoir temperature transients modelling works are listed, chronologically.

In this study, the transient wellbore temperature behaviors in wellbores under nonisothermal single-phase liquid flow conditions in oil reservoirs are modeled and interpreted. The analytical equations developed in this study provide information content of transient-temperature measurement made under single-phase flow of slightly compressible fluid for a vertical wellbore across from producing horizon during drawdown and buildup tests.

## **1.2 Problem Statement**

Until now, pressure changes were modeled by researchers in order to understand wellbore and reservoir characterization; however, researchers have not studied sufficiently about transient temperature changes as a function of the gauge depth inside the wellbore for both production and buildup periods during well tests because of lack of analytical studies. In this study, we model and interpret transient wellbore temperature behaviors as a function of gauge position in wellbores under nonisothermal single-phase liquid flow conditions in oil reservoirs.

## **1.3 Objective of Research**

The main goal of this study is to model transient wellbore temperature behaviors for a single-phase liquid flow under nonisothermal conditions analytically. New analytical and semi-analytical solutions depend on a coupled wellbore/reservoir thermal model are provided to interrogate the transient temperature measurement information in the vertical wellbore as a function of the gauge depth. This measurement is performed across from producing horizon or at a gauge depth above it during drawdown and buildup tests. Based on temperature-derivative and straight line methods, new interpretation methodologies of sandface and wellbore transient temperature information is investigated. Some considerations are slightly compressible, single-phase, and homogenous infinite-acting reservoir system with skin effect. Also, Joule Thomson heating/cooling, adiabatic fluid expansion, conduction, and convection impacts are accounted for in the analytical solutions.

## 1.4 Significance of the Study

Like pressure data, transient temperature data provide many information about reservoir characterizations. Until today, researchers have tried various methods in order to analyze transient temperature data analytically or numerically. In this study, we model analytically transient temperature behaviors in wellbore using mass and momentum balance equations, and also compare results with RUBIS as Sui did in his thesis. The significance of the work is that analytical steady-state and transient

## 1.5 Scopes of the Study

Main assumptions for wellbore are below:

- 1D radial flow, and single phase oil with irreducible-water saturation.
- Slightly compressible fluids (oil and water) are immiscible.
- Darcy's Law governs fluid flow in each zone.
- Reservoir parameters and thermal properties of fluid and rock are constant, do not vary with pressure and temperature namely.
- The well is vertical and fully perforated.
- The solid matrix which is rigid (zero velocity), oil, and connate water are in a local thermal equilibrium ( $T_s = T_w = T_o = T$ ).
- Gravity and capillary effects are ignored.

In this work, the subscripts  $o$ ,  $w$ ,  $s$ ,  $r$  and  $t$  refer to oil phase, water phase, solid matrix, effective rock, and total system properties, respectively.

## 1.6 Thesis Structure

Thesis structure can be defined as following steps:

In Chapter 2, a general derivation of conventional wellbore storage model including changes of density and compressibility with  $p$  and  $T$  will be given, and then reduced under certain assumptions. Also, a general derivation of mass and momentum balance equations will be given with specific considerations.

In Chapter 3, derivation of transient wellbore thermal energy equation will be provided using overall heat transfer coefficient, correlations for dimensionless heat transfer

functions, and earth geothermal gradient modeling. Then, transient and steady-state wellbore temperature solutions will be derived.

In Chapter 4, the solutions in Laplace space for variable-rate case including constant-rate and buildup periods derived by Kocak (2017) will be given as they are necessary to compute transient wellbore pressure and temperature solutions given in this study. Besides, it is stated that using the Crump algorithm for inversion of Laplace space solutions inverted by using the Stehfest algorithm.

In Chapter 5, the behaviors of sandface and wellbore flow rate, pressure, and temperature distributions will be investigated for production and buildup cases.

In Chapter 6, the impact of various parameters such as gauge location, production flow rate, geothermal gradient, earth conductivity and diffusivity, and well length on temperature solutions will be investigated.

In Chapter 7, we will provide some interpretation and analysis methodology for predicting parameters such as permeability, skin, J-T coefficient, thermal conductivity of earth and formation, etc from transient wellbore temperatures along with transient wellbore pressure data.

In Chapter 8, conclusions of the study and recommendations for future work will be present

## 2. WELLBORE MASS AND MOMENTUM FLUID FLOW MODEL EQUATIONS

### 2.1 Conventional Wellbore Storage Model

**Mass Balance Equation:** In this section, a general derivation of conventional wellbore storage model including changes of density and compressibility with  $p$  and  $T$  will be given.

Here, we present the derivation of the mass balance equation by considering the flow of a slightly-compressible fluid in a linearly elastic walls of a vertical pipe (see Fig. 1) with a constant cross-section over the length of a pipe. Furthermore, we consider a small control volume and assume that the flow is one dimensional. The radial velocity due to expansion and contraction of the pipe wall is small and can be ignored.

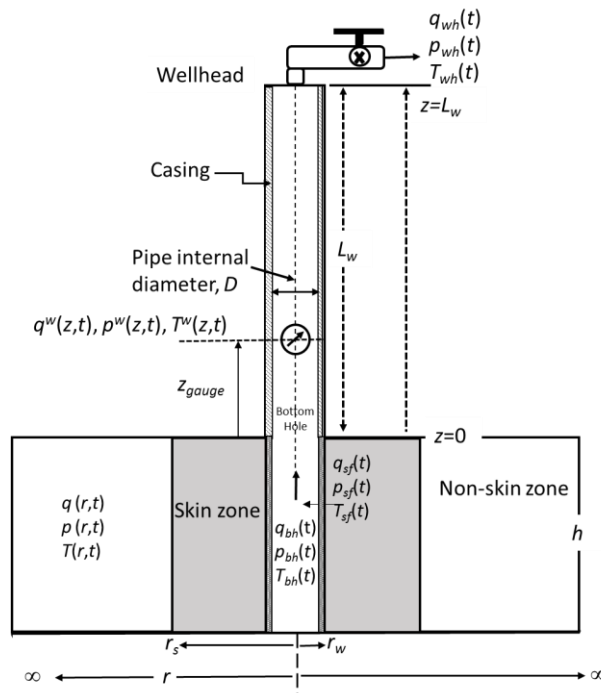


**Figure 2.1:** A cylindrical homogeneous reservoir with a vertical well where the well head flow is controlled, and the bottomhole flow rate pressure and temperature are measured. Note that locations of pressure and temperature gauges may be at different horizons in the wellbore.

Consider the figure shown in Fig. 1, where the distance  $z$ , velocity  $u^w(z,t)$  are considered positive in the upward direction, and fluid discharge  $q^w(z,t)$ . The mass balance equation can be given as:

$$\frac{\partial(\rho^w A^w)}{\partial t} + \frac{\partial(\rho^w A^w u^w)}{\partial z} = 0 \quad (2.1)$$

The cross-sectional area  $A^w$  along the  $z$ -direction, may change with  $z$  and  $t$ , i.e.,  $A^w(z, t)$ , because of pipe elasticity (or strain). Also note that we can express the second term in the left-hand side of Eq. 2.1 in terms of flow rate;  $q^w(z, t)$  because  $q^w(z, t) = u^w(z, t)A(t)$ . Hence, Eq. 2.1 can be expressed as:

$$\frac{\partial(\rho^w A^w)}{\partial t} + \frac{\partial(\rho^w q^w)}{\partial z} = 0 \quad (2.2)$$

As density in the wellbore is a function of both pressure and temperature and for the purpose of generality, we assume an elastic pipe where its cross-sectional area changes only with pressure and hence with time. So, Eq. 2.2 can be expressed as:

$$A^w \frac{\partial \rho^w}{\partial t} + \rho^w \frac{\partial A^w}{\partial t} + \frac{\partial(\rho^w q^w)}{\partial z} = 0 \quad (2.3)$$

Using the chain rule for time derivative of density which is a function of both temperature and pressure gives:

$$\frac{\partial \rho^w}{\partial t} = \left( \frac{\partial \rho^w}{\partial p^w} \right)_{T^w} \left( \frac{\partial p^w}{\partial t} \right) + \left( \frac{\partial \rho^w}{\partial T^w} \right)_{p^w} \left( \frac{\partial T^w}{\partial t} \right) \quad (2.4)$$

Using the definitions of isothermal fluid compressibility and isobaric thermal expansion coefficients, which are defined by

$$c^w = \frac{1}{\rho^w} \left( \frac{\partial \rho^w}{\partial p^w} \right)_{T^w} \quad (2.5)$$

and

$$\beta^w = -\frac{1}{\rho^w} \left( \frac{\partial \rho^w}{\partial T^w} \right)_{p^w} \quad (2.6)$$

in Eq. 2.4 gives

$$\frac{\partial \rho^w}{\partial t} = \rho^w \left( c^w \frac{\partial p^w}{\partial t} - \beta^w \frac{\partial T^w}{\partial t} \right) \quad (2.7)$$

Furthermore, we use chain rule for the time derivative of the cross-sectional area in Eq. 2.3:

$$\frac{\partial A^w}{\partial t} = \left( \frac{\partial A^w}{\partial p^w} \right)_{T^w} \left( \frac{\partial p^w}{\partial t} \right) \quad (2.8)$$

Using Eqs. 2.7 and 2.8 in Eq. 2.3 gives:

$$A^w \rho^w \left( c^w \frac{\partial p^w}{\partial t} - \beta^w \frac{\partial T^w}{\partial t} \right) + \rho^w \left( \frac{\partial A^w}{\partial p^w} \right)_{T^w} \left( \frac{\partial p^w}{\partial t} \right) + \frac{\partial(\rho^w q^w)}{\partial z} = 0 \quad (2.9)$$

Furthermore, we can expand the third in the LHS of Eq. 2.9 as:

$$\frac{\partial(\rho^w q^w)}{\partial z} = \rho^w \frac{\partial q^w}{\partial z} + q^w \frac{\partial \rho^w}{\partial z} \quad (2.10)$$

Where the second derivative term in the RHS of Eq. 2.10 can be expressed by using the chain rule as:

$$\frac{\partial \rho^w}{\partial z} = \left( \frac{\partial \rho^w}{\partial p^w} \right)_{T^w} \frac{\partial p^w}{\partial z} + \left( \frac{\partial \rho^w}{\partial T^w} \right)_{p^w} \frac{\partial T^w}{\partial z} \quad (2.11)$$

Using the definitions of isothermal compressibility (Eq. 2.5) and isobaric thermal expansion coefficient (Eq. 2.6) in Eq. 2.11, Eq. 2.11 can be expressed as:

$$\frac{\partial \rho^w}{\partial z} = \rho^w \left( c^w \frac{\partial p^w}{\partial z} - \beta^w \frac{\partial T^w}{\partial z} \right) \quad (2.12)$$

Now using Eq. 2.12 in Eq. 2.10 gives:

$$\frac{\partial(\rho^w q^w)}{\partial z} = \rho^w \frac{\partial q^w}{\partial z} + \rho^w q^w \left( c^w \frac{\partial p^w}{\partial z} - \beta^w \frac{\partial T^w}{\partial z} \right) \quad (2.13)$$

Substituting Eq. 2.13 in Eq. 2.9 gives:

$$\begin{aligned} A^w \rho^w \left( c^w \frac{\partial p^w}{\partial t} - \beta^w \frac{\partial T^w}{\partial t} \right) + \rho^w \left( \frac{\partial A^w}{\partial p^w} \right)_{T^w} \left( \frac{\partial p^w}{\partial t} \right) + \rho^w \frac{\partial q^w}{\partial z} + \\ \rho^w q^w \left( c^w \frac{\partial p^w}{\partial z} - \beta^w \frac{\partial T^w}{\partial z} \right) = 0 \end{aligned} \quad (2.14)$$

Eliminating densities from Eq. 2.14 result in:

$$\begin{aligned} A^w \left( c^w \frac{\partial p^w}{\partial t} - \beta^w \frac{\partial T^w}{\partial t} \right) + \left( \frac{\partial A^w}{\partial p^w} \right)_{T^w} \left( \frac{\partial p^w}{\partial t} \right) + \frac{\partial q^w}{\partial z} + q^w \left( c^w \frac{\partial p^w}{\partial z} - \right. \\ \left. \beta^w \frac{\partial T^w}{\partial z} \right) = 0 \end{aligned} \quad (2.15)$$

We can express Eq. 15 in terms of the bulk modulus of the fluid, which is equal to the inverse of the isothermal compressibility of the fluid; that is,

$$K^w = \frac{1}{c^w} \quad (2.16)$$

The variation of cross-sectional area with  $p$  can be related to the Young's modulus ( $E$ ) of the pipe and as given by:

$$\left(\frac{\partial A^w}{\partial p^w}\right)_{T^w} = \frac{D}{eE} A^w \quad (2.17)$$

where  $e$  is the wall thickness of the pipe and  $D$  is the inner diameter of the pipe.

Now using the expressions given by Eq. 2.16 and 2.17 in Eq. 2.16-2.5 gives:

$$A^w \left( \frac{1}{K^w} \frac{\partial p^w}{\partial t} - \beta^w \frac{\partial T^w}{\partial t} \right) + \frac{D}{eE} A^w \left( \frac{\partial p^w}{\partial t} \right) + \frac{\partial q^w}{\partial z} + q^w \left( \frac{1}{K^w} \frac{\partial p^w}{\partial z} - \beta^w \frac{\partial T^w}{\partial z} \right) = 0 \quad (2.18)$$

Eq. 2.18 can be rearranged as:

$$A^w \left( \frac{1}{K^w} + \frac{D}{eE} \right) \frac{\partial p^w}{\partial t} + \frac{q^w}{K^w} \frac{\partial p^w}{\partial z} - A^w \beta^w \frac{\partial T^w}{\partial t} - \beta^w q^w \frac{\partial T^w}{\partial z} + \frac{\partial q^w}{\partial z} = 0 \quad (2.19)$$

Recall that the sonic velocity is defined

$$a = \sqrt{\frac{K^w}{\rho^w [1 + DK^w (eE)^{-1}]}} \quad (2.20)$$

and is also the speed at which the pressure waves generated by water hammer travel in the pipe (also referred to as velocity of water-hammer wave in the fluid). Eq. 2.20 can be rearranged as:

$$\frac{1}{a^2} = \frac{\rho^w}{K^w} + \frac{\rho^w D}{eE} \quad (2.21)$$

Using Eq. 2.21 in Eq. 2.19 gives:

$$\frac{A^w}{a^2 \rho^w} \frac{\partial p^w}{\partial t} + \frac{q^w}{K^w} \frac{\partial p^w}{\partial z} - A^w \beta^w \frac{\partial T^w}{\partial t} - \beta^w q^w \frac{\partial T^w}{\partial z} + \frac{\partial q^w}{\partial z} = 0 \quad (2.22)$$

Some remarks are in order for Eq. 2.22:

1. If we have an isothermal flow, Eq. 2.22 reduces to:

$$\frac{A^w}{a^2 \rho^w} \frac{\partial p^w}{\partial t} + \frac{q^w}{K^w} \frac{\partial p^w}{\partial z} + \frac{\partial q^w}{\partial z} = 0 \quad (2.23)$$

or

$$\frac{\partial p^w}{\partial t} + \frac{q^w}{K^w} \frac{a^2 \rho^w}{A^w} \frac{\partial p^w}{\partial z} + \frac{a^2 \rho^w}{A^w} \frac{\partial q^w}{\partial z} = 0 \quad (2.24)$$

Chaudhry (2014) states that in most of the engineering calculations, the convective acceleration term, i.e., the second term in Eq. 2.23 (or 2.24) is small as compared to the other terms so that Eq. 2.24 is approximated by

$$\frac{\partial p^w}{\partial t} + \frac{a^2 \rho^w}{A^w} \frac{\partial q^w}{\partial z} = 0 \quad (2.25)$$

2. For a rigid pipe, we have

$$\left(\frac{\partial A^w}{\partial p^w}\right)_{T^w} = 0 \quad (2.26)$$

So, to obtain the mass balance equation for a rigid pipe, to satisfy Eq. 2.24, we set  $D(eE)^{-1}$  in Eq. 2.20, so that the sonic velocity becomes

$$a = \sqrt{\frac{K^w}{\rho^w}} = \sqrt{\frac{1}{c^w \rho^w}} = \sqrt{\left(\frac{dp^w}{d\rho^w}\right)_{T^w}} \quad (2.27)$$

or

$$a^2 = \frac{K^w}{\rho^w} = \left(\frac{dp^w}{d\rho^w}\right)_{T^w} = \frac{1}{c^w \rho^w} \quad (2.28)$$

It should be noted that although we will consider nonisothermal flow in the wellbore when solving thermal energy-balance, we will assume that the temperature changes with time and space in mass and momentum balance equations could be neglected when we couple the mass and momentum equations in the wellbore. This is a realistic assumption because the temperature changes with time and in the vertical directions are quite small as compared to the pressure changes with time and in the vertical direction in Eq. 2.22. So, we consider the following approximate mass balance equation which follows directly from Eq. 2.22 by neglecting the time and space derivatives of temperature in Eq. 2.22 and the convective term in Eq. 2.22 as:

$$\frac{A^w}{a^2 \rho^w} \frac{\partial p^w}{\partial t} + \frac{\partial q^w}{\partial z} = 0 \quad (2.29)$$

Furthermore, we assume a rigid-pipe, and hence, Eq. 2.29 can be expressed as:

$$\frac{\partial p^w}{\partial t} + \frac{1}{A^w c^w} \frac{\partial q^w}{\partial z} = 0 \quad (2.30)$$

The classical wellbore storage model used for accounting compressive type wellbore storage effects under single-phase flow assumption is based on only the mass-balance equation given by Eq. 2.30.

Integration of Eq. 2.30 with respect to  $z$ ,

$$\int A^w c^w \frac{\partial p^w}{\partial t} = - \int_{q_{sf}}^{q_{wh}} \frac{\partial q^w}{\partial z} \quad (2.31)$$

$$A^w c^w z \frac{\partial p^w}{\partial t} = -(q_{wh}(t) - q_{sf}(t)) \quad (2.32)$$

$$q_{sf}(t) = q_{wh}(t) + A^w c^w z \frac{\partial p^w}{\partial t} \quad (2.33)$$

We know that volume ( $V^w$ ) equals multiplying of cross-sectional area ( $A$ ) and wellbore length ( $z$ ).

$$q_{sf}(t) = q_{wh}(t) + V^w c^w \frac{\partial p^w}{\partial t} \quad (2.34)$$

Definition of wellbore storage is that if some portion of the production is owing to expansion or compression of fluid in wellbore after a rate change, this effect is the wellbore storage. Its formula can be given as shown in eq. (2.35):

$$C = c^w V^w \quad (2.35)$$

The final equation is:

$$q_{sf}(t) = q_{wh}(t) + C \frac{\partial p^w}{\partial t} \quad (2.36)$$

where  $C$  is the wellbore storage coefficient which is in  $\text{m}^3/\text{Pa}$ . It is assumed to be constant, and same for both drawdown and buildup periods.

If we take the Laplace transform of Eq. 2.36, given by

$$\begin{aligned} \bar{q}_{sf}(s) &= \bar{q}_{wh}(s) + C[s\bar{p}_{bh} - p_{bh}(t = 0)] \\ &= \bar{q}_{wh}(s) + C[s\bar{p}_{bh} - p^w(z = 0, t = 0)] \end{aligned} \quad (2.37)$$

In the Eq. 2.37,  $s$  represents the Laplace transform variable.

In this work, we assume that the formation is in the hydraulic equilibrium with the wellbore. Superscripted to  $w$  refers to the wellbore properties.

To compute bottomhole pressure  $p_{bh}$  as a function of time, the solutions of a composite reservoir fluid flow model for a line-sink or finite wellbore as presented in SPE-181710 Onur et al. (2016) are used. In Laplace space in terms of the specified wellhead flow rate and the wellbore storage coefficient, Eq. 2.37 gives the solution for sandface or bottomhole flow rate:

$$\bar{q}_{sf}(s) = \frac{\bar{q}_{wh}(s)}{[1+C_s\Psi(r_w,s)]} \quad (2.38)$$

where  $\Psi(r_w, s)$  is referred to the unit impulse response (Kuchuk et al.2010). It is given in SPE-181710 for a finite wellbore and for a line sink well, respectively:

$$\Psi(r_w, s) = \frac{1}{2\pi\kappa_s h r_w} \sqrt{\frac{\eta_s}{s}} \frac{[K_0(r_w \sqrt{\frac{s}{\eta_s}}) + \Omega(u)I_0(r_w \sqrt{\frac{s}{\eta_s}})]}{[K_1(r_w \sqrt{\frac{s}{\eta_s}}) + \Omega(u)I_1(r_w \sqrt{\frac{s}{\eta_s}})]} \quad (2.39)$$

and

$$\Psi(r_w, s) = \frac{1}{2\pi\kappa_s h} \left[ K_0\left(r_w \sqrt{\frac{s}{\eta_s}}\right) + \Omega(s)I_0\left(r_w \sqrt{\frac{s}{\eta_s}}\right) \right] \quad (2.40)$$

The bottomhole pressure  $p_{bh}$  can be defined in the Laplace space as:

$$\bar{p}_{bh}(s) = \frac{p^w(z=0,t=0)}{s} - \frac{\bar{q}_{wh}(s)\Psi(r_w,s)}{[1+C_s\Psi(r_w,s)]} \quad (2.41)$$

$K_0$ ,  $I_0$ ,  $K_1$ , and  $I_1$  are the Bessel Functions.

## 2.2 Momentum Model

For a single-phase slightly-compressible fluid flow, the momentum equation for a slanted wellbore of angle  $\theta$  (is the angle that the conduit makes with the horizontal, considered positive for the conduit sloping upward in the downstream direction, see Chaudhry 2014. Note for a vertical well  $\theta = 90^\circ$ ) taking into account the specific contributions of pressure forces, friction loss, and gravity can be given as:

$$\frac{\partial(\rho^w u^w A^w)}{\partial t} + \frac{\partial[\rho^w A^w (u^w)^2]}{\partial z} + A^w \frac{\partial p^w}{\partial z} + \rho^w g A^w \sin \theta + \tau_0 \pi D = 0 \quad (2.42)$$

where  $\tau_0$  is the shear stress exerted by the conduit (pipe) walls on the flowing fluid. We assume that the energy losses for a given flow velocity during the transient state are the same as those for steady state flows at that velocity. If we use the Darcy-Weishbach friction equation for computing the friction losses, the wall shear stress can be given by

$$\tau_0^w = \frac{1}{8} \rho^w f u^w |u^w| \quad (2.43)$$

Where  $f$  represents the Darcy-Weishbach friction factor. Note that we are writing  $(u^w)^2$  as  $u^w |u^w|$  to permit the reverse flow.

Substitution of Eq. 2.43 into Eq. 2.42 and the expansion of the terms in parantheses yield:

$$\begin{aligned} u^w \frac{\partial(\rho^w A^w)}{\partial t} + \rho^w A^w \frac{\partial u^w}{\partial t} + \rho^w A^w u^w \frac{\partial u^w}{\partial z} + u^w \frac{\partial(\rho^w A^w u^w)}{\partial z} + A^w \frac{\partial p^w}{\partial z} + \rho^w g \\ A^w \sin \theta + \frac{1}{8} \frac{\pi D^2}{4} \frac{4}{\pi D^2} \rho^w f u^w |u^w| \pi D = 0 \end{aligned} \quad (2.44)$$

Because  $A^w = \pi D^2/4$ , Eq. 2.44 can be written as:

$$\begin{aligned} u^w \frac{\partial(\rho^w A^w)}{\partial t} + \rho^w A^w \frac{\partial u^w}{\partial t} + \rho^w A^w u^w \frac{\partial u^w}{\partial z} + u^w \frac{\partial(\rho^w A^w u^w)}{\partial z} + A^w \frac{\partial p^w}{\partial z} + \rho^w g \\ A^w \sin \theta + \frac{A^w \rho^w f u^w |u^w|}{2D} = 0 \end{aligned} \quad (2.45)$$

The rearrangement of the terms of this equation gives:

$$\begin{aligned} u^w \left[ \frac{\partial(\rho^w A^w)}{\partial t} + \frac{\partial(\rho^w A^w u^w)}{\partial z} \right] + \rho^w A^w \frac{\partial u^w}{\partial t} + \rho^w A^w u^w \frac{\partial u^w}{\partial z} + A^w \frac{\partial p^w}{\partial z} + \rho^w g \\ A^w \sin \theta + \frac{A^w \rho^w f u^w |u^w|}{2D} = 0 \end{aligned} \quad (2.46)$$

Based on the continuity equation (Eq. 2.1) the sum of the two terms inside the brackets of Eq. 2.46 is zero. Hence, dropping the terms inside the brackets gives

$$\rho^w A^w \frac{\partial u^w}{\partial t} + \rho^w A^w u^w \frac{\partial u^w}{\partial z} + A^w \frac{\partial p^w}{\partial z} + \rho^w g A^w \sin \theta + \frac{A^w \rho^w f u^w |u^w|}{2D} = 0 \quad (2.47)$$

and dividing Eq. 2.47 by  $\rho^w A^w$  gives:

$$\frac{\partial u^w}{\partial t} + u^w \frac{\partial u^w}{\partial z} + \frac{1}{\rho^w} \frac{\partial p^w}{\partial z} + g \sin \theta + \frac{f u^w |u^w|}{2D} = 0 \quad (2.48)$$

For a rigid pipe, we can express Eq. 2.48 in terms of volumetric flow rate as:

$$\frac{1}{A^w} \frac{\partial q^w}{\partial t} + \frac{q^w}{(A^w)^2} \frac{\partial q^w}{\partial z} + \frac{1}{\rho^w} \frac{\partial p^w}{\partial z} + g \sin \theta + \frac{f q^w |q^w|}{2(A^w)^2 D} = 0 \quad (2.49)$$

For a laminar flow, the friction factor is given by:

$$f = \frac{64 \mu^w}{\rho^w u^w D} = \frac{64 \nu^w}{u^w D} \quad (2.50)$$

where  $\nu^w$  is the kinematic viscosity. For laminar flow, with the use of Eq. 2.50 in Eq. 2.49, Eq. 2.49 becomes:

$$\frac{1}{A^w} \frac{\partial q^w}{\partial t} + \frac{q^w}{(A^w)^2} \frac{\partial q^w}{\partial z} + \frac{1}{\rho^w} \frac{\partial p^w}{\partial z} + g \sin \theta + \frac{64\nu^w}{2A^w D^2} q^w = 0 \quad (2.51)$$

Defining

$$R = \frac{32\nu^w}{D^2} \quad (2.52)$$

then using expression given by Eqs. 2.52 in Eq. 2.51 gives:

$$\frac{1}{A^w} \frac{\partial q^w}{\partial t} + \frac{q^w}{(A^w)^2} \frac{\partial q^w}{\partial z} + \frac{1}{\rho^w} \frac{\partial p^w}{\partial z} + g \sin \theta + \frac{Rq^w}{A^w} = 0 \quad (2.53)$$

Neglecting the convective acceleration term, i.e., the second term in Eq. 2.53, we have a simplified version of Eq. 2.53 as:

$$\frac{1}{A^w} \frac{\partial q^w}{\partial t} + \frac{1}{\rho^w} \frac{\partial p^w}{\partial z} + g \sin \theta + \frac{Rq^w}{A^w} = 0 \quad (2.54)$$

Multiply both sides by the cross-sectional area gives:

$$\frac{\partial q^w}{\partial t} + \frac{A^w}{\rho^w} \frac{\partial p^w}{\partial z} + A^w g \sin \theta + Rq^w = 0 \quad (2.55)$$

Furthermore, consider a vertical wellbore,  $\theta = 90^\circ$ , then Eq. 2.55 becomes:

$$\frac{\partial q^w}{\partial t} + \frac{A^w}{\rho^w} \frac{\partial p^w}{\partial z} + A^w g + Rq^w = 0 \quad (2.56)$$

It is a common practice in hydraulic engineering to compute pressures in the pipeline in terms of the hydraulic head,  $H$ , above a specified datum, i.e.,

$$p^w = \rho^w g (H - z) \quad (2.57)$$

The partial derivative of  $p^w$  given by Eq. 2.57 with respect to  $z$  is

$$\frac{\partial p^w}{\partial z} = \rho^w g \left( \frac{\partial H}{\partial z} - 1 \right) \quad (2.58)$$

Using Eq. 2.58 in Eq. 2.56 gives:

$$\frac{\partial q^w}{\partial t} + A^w g \left( \frac{\partial H}{\partial z} - 1 \right) + A^w g + Rq^w = 0 \quad (2.59)$$

Cancelling  $A^w g$  terms:

$$\frac{\partial q^w}{\partial t} + A^w g \frac{\partial H}{\partial z} + Rq^w = 0 \quad (2.60)$$

Since we deal with pressure, the hydraulic head is transformed into hydraulic pressure in the well denoted by  $p^w = \rho^w g H$ , then using this in Eq. 2.60 gives:

$$\frac{\partial q^w}{\partial t} + A^w g \frac{\partial (p^w / \rho^w g)}{\partial z} + Rq^w = 0 \quad (2.61)$$

Neglecting the variation of density along  $z$ , momentum equation reduces to:

$$\frac{\partial q^w}{\partial t} + \frac{A^w}{\rho^w} \frac{\partial p^w}{\partial z} + Rq^w = 0 \quad (2.62)$$

For solutions of mass and momentum balance equations, we follow Mansori et al. (SPE 176301) approach. Earlier it is shown that the mass balance and momentum balance equations for a vertical wellbore where we have flow of slightly compressible fluid under laminar flow conditions can be written as:

$$\frac{\partial p^w}{\partial t} + \frac{1}{A^w c^w} \frac{\partial q^w}{\partial z} = 0 \quad (2.63)$$

and

$$\frac{\partial q^w}{\partial t} + \frac{A^w}{\rho^w} \frac{\partial p^w}{\partial z} + Rq^w = 0 \quad (2.64)$$

We can combine Eqs. 2.63 and 2.64 (by eliminating pressure  $p^w$ ). Let's take the derivative of Eq. 2.63 with respect to  $z$  and the derivative of the second equation with respect to time to obtain the following equations, respectively,

$$\frac{\partial^2 p^w}{\partial t \partial z} + \frac{1}{A^w c^w} \frac{\partial^2 q^w}{\partial z^2} = 0 \quad (2.65)$$

and

$$\frac{\partial^2 q^w}{\partial t^2} + \frac{A^w}{\rho^w} \frac{\partial^2 p^w}{\partial t \partial z} + R \frac{\partial q^w}{\partial t} = 0 \quad (2.66)$$

Multiplying the first equation by  $A^w/\rho^w$  gives:

$$\frac{A^w}{\rho^w} \frac{\partial^2 p^w}{\partial t \partial z} + \frac{1}{\rho^w c^w} \frac{\partial^2 q^w}{\partial z^2} = 0 \quad (2.67)$$

Subtracting Eq. 2.67 from Eq. 2.66 gives:

$$\frac{\partial^2 q^w}{\partial t^2} + R \frac{\partial q^w}{\partial t} - \frac{1}{\rho^w c^w} \frac{\partial^2 q^w}{\partial z^2} = 0 \quad (2.68)$$

or can be rearranged as:

$$\frac{\partial^2 q^w}{\partial z^2} - \rho^w c^w \frac{\partial^2 q^w}{\partial t^2} - \rho^w c^w R \frac{\partial q^w}{\partial t} = 0 \quad (2.69)$$

We solve Eq. 2.69 subject to the following ICs. It is assumed that the well does not produce at time  $t \leq 0$ :

$$q^w(z, 0) = 0, \text{ for } 0 \leq z \leq L_w \quad (2.70)$$

$$\frac{\partial q^w}{\partial z}(z, 0) = 0, \text{ for } 0 \leq z \leq L_w \quad (2.71)$$

Taking the Laplace transform of Eq. 2.69 gives:

$$\frac{\partial^2 \bar{q}^w}{\partial z^2} - \rho^w c^w \left[ s^2 \bar{q}^w - s q^w(z, t=0) - \frac{\partial q^w(z, t=0)}{\partial t} \right] - \rho^w c^w R [s \bar{q}^w - q^w(z, t=0)] = 0 \quad (2.72)$$

Using Eqs. 2.70 and 2.71 in Eq. 2.72 gives:

$$\frac{\partial^2 \bar{q}^w}{\partial z^2} - \rho^w c^w (s^2 \bar{q}^w) - \rho^w c^w R (s \bar{q}^w) = 0 \quad (2.73)$$

or

$$\frac{\partial^2 \bar{q}^w}{\partial z^2} - \rho^w c^w (s^2 + Rs) \bar{q}^w = 0 \quad (2.74)$$

Eq. 2.74 is a second order homogeneous ODE. Its general solution can be expressed as:

$$\bar{q}^w(s) = M_1 \sinh[\sqrt{\rho^w c^w (s^2 + Rs)} z] + M_2 \cosh[\sqrt{\rho^w c^w (s^2 + Rs)} z] \quad (2.75)$$

where  $M_1$  and  $M_2$  are arbitrary constants to be determined from the boundary conditions. If Eq. 2.63 is transformed into the Laplace domain, we obtain:

$$s\bar{p}^w - p^w(z, t = 0) + \frac{1}{A^w c^w} \frac{\partial \bar{q}^w}{\partial z} = 0 \quad (2.76)$$

Taking derivative of Eq. 2.75 with respect to  $z$  gives:

$$\begin{aligned} \frac{\partial \bar{q}^w(s)}{\partial z} = & M_1 \sqrt{\rho^w c^w (s^2 + Rs)} \cosh[\sqrt{\rho^w c^w (s^2 + Rs)} z] + \\ & M_2 \sqrt{\rho^w c^w (s^2 + Rs)} \sinh[\sqrt{\rho^w c^w (s^2 + Rs)} z] \end{aligned} \quad (2.77)$$

Using Eq. 2.77 in Eq. 2.76 and the rearranging the resulting equation, we have:

$$\begin{aligned} \bar{p}^w = & \frac{p^w(z, t=0)}{s} - \\ & \frac{1}{A^w c^w} \left\{ M_1 \sqrt{\rho^w c^w (s^2 + Rs)} \cosh[\sqrt{\rho^w c^w (s^2 + Rs)} z] + \right. \\ & \left. M_2 \sqrt{\rho^w c^w (s^2 + Rs)} \sinh[\sqrt{\rho^w c^w (s^2 + Rs)} z] \right\} \end{aligned} \quad (2.78)$$

Two boundary conditions are required to find  $M_1$  and  $M_2$  in Eqs. 2.75 and 2.78. At each side of the wellbore, either flow rate or pressure can be specified. For example, in a well test, the choke controls the flow rate at the wellhead and the reservoir response determines the pressure at the bottomhole; so, we can take wellhead specified rate,  $q_{wh}(t)$ , and the bottomhole pressure  $p_{bh}(t)$  as boundary conditions.

So, evaluating Eq. 2.75 at  $z = L_w$  gives:

$$M_1 \sinh[\sqrt{\rho^w c^w (s^2 + Rs)} L_w] + M_2 \cosh[\sqrt{\rho^w c^w (s^2 + Rs)} L_w] = \bar{q}_{wh} \quad (2.79)$$

$$\begin{aligned} \frac{p^w(z=0, t=0)}{s} - \frac{1}{A^w c^w} \left\{ M_1 \sqrt{\rho^w c^w (s^2 + Rs)} \cosh[\sqrt{\rho^w c^w (s^2 + Rs)} 0] + \right. \\ \left. M_2 \sqrt{\rho^w c^w (s^2 + Rs)} \sinh[\sqrt{\rho^w c^w (s^2 + Rs)} 0] \right\} = \bar{p}_{bh} \end{aligned} \quad (2.80)$$

or

$$\frac{p^w(z=0, t=0)}{s} - \frac{M_1 \sqrt{\rho^w c^w (s^2 + Rs)}}{A^w c^w} = \bar{p}_{bh} \quad (2.81)$$

So, Eq. 2.81 determines  $M_1$  as:

$$\frac{M_1 \sqrt{\rho^w c^w (s^2 + Rs)}}{A^w c^w} = \frac{p^w(z=0, t=0)}{s} - \bar{p}_{bh} \quad (2.82)$$

or

$$M_1 = \frac{A^w c^w}{\sqrt{\rho^w c^w (s^2 + Rs)}} \left[ \frac{p^w(z=0, t=0)}{s} - \bar{p}_{bh} \right] \quad (2.83)$$

Using Eq. 2.83 in Eq. 2.79 determines  $M_2$  as:

$$M_2 = \bar{q}_{wh} - \frac{A^w c^w \tanh[\sqrt{\rho^w c^w (s^2 + Rs)} L_w]}{\sqrt{\rho^w c^w (s^2 + Rs)}} \left[ \frac{p^w(z=0, t=0)}{s} - \bar{p}_{bh} \right] \quad (2.84)$$

Using Eqs. 2.83 and 2.84 in Eq. 2.75 gives the flow rate profile in Laplace space:

$$\bar{q}^w(z, s) = \frac{A^w c^w \left[ \frac{p^w(z=0, t=0)}{s} - \bar{p}_{bh} \right]}{\sqrt{\rho^w c^w (s^2 + Rs)}} \sinh[\sqrt{\rho^w c^w (s^2 + Rs)} z] + \left\{ \bar{q}_{wh} - \frac{A^w c^w \tanh[\sqrt{\rho^w c^w (s^2 + Rs)} L_w]}{\sqrt{\rho^w c^w (s^2 + Rs)}} \left[ \frac{p^w(z=0, t=0)}{s} - \bar{p}_{bh} \right] \right\} \cosh[\sqrt{\rho^w c^w (s^2 + Rs)} z] \quad (2.85)$$

or

$$\begin{aligned} \bar{q}^w(z, s) = & \frac{A^w c^w \left[ \frac{p^w(z=0, t=0)}{s} - \bar{p}_{bh} \right]}{\sqrt{\rho^w c^w (s^2 + Rs)}} \left\{ \sinh[\sqrt{\rho^w c^w (s^2 + Rs)} z] - \right. \\ & \left. \tanh[\sqrt{\rho^w c^w (s^2 + Rs)} L_w] \cosh[\sqrt{\rho^w c^w (s^2 + Rs)} z] \right\} \\ & + \bar{q}_{wh} [\sqrt{\rho^w c^w (s^2 + Rs)} z] \end{aligned} \quad (2.86)$$

Using Eqs. 2.83 and 2.84 in Eq. 2.78 gives the pressure profile in Laplace space:

$$\begin{aligned} \bar{p}^w = & \frac{p^w(z=0, t=0)}{s} - \frac{1}{A^w c^w} \left\{ \frac{A^w c^w}{\sqrt{\rho^w c^w (s^2 + Rs)}} \left[ \frac{p^w(z=0, t=0)}{s} - \right. \right. \\ & \left. \left. \bar{p}_{bh} \right] \sqrt{\rho^w c^w (s^2 + Rs)} \cosh[\sqrt{\rho^w c^w (s^2 + Rs)} z] + \left\{ \bar{q}_{wh} - \right. \right. \\ & \left. \left. \frac{A^w c^w \tanh[\sqrt{\rho^w c^w (s^2 + Rs)} L_w]}{\sqrt{\rho^w c^w (s^2 + Rs)}} \left[ \frac{p^w(z=0, t=0)}{s} - \right. \right. \right. \\ & \left. \left. \bar{p}_{bh} \right] \right\} \sqrt{\rho^w c^w (s^2 + Rs)} \sinh[\sqrt{\rho^w c^w (s^2 + Rs)} z] \left. \right\} \end{aligned} \quad (2.87)$$

Important Remarks on Eqs. 2.86 and 2.87:

1. In Eqs. 2.86 and 2.87,  $q_{wh}$  is the surface or wellhead flow rate in Laplace domain, as we will consider constant-rate drawdown followed by buildup, then we can express  $q_{wh}$  as:

$$q_{wh}(t) = [1 - H(t - t_p)]q_{sc} = \begin{cases} q_{sc} & t < t_p \\ 0 & t > t_p \end{cases} \quad (2.88)$$

Where  $q_{sc}$  is a constant rate, and  $t_p$  is the producing time before shut-in. The Laplace transform of Eq. 2.88 is given by:

$$\bar{q}_{wh}(s) = [1 - e^{-st_p}] \frac{q_{sc}}{s} \quad (2.89)$$

2. In Eqs. 2.86 and 2.87,  $p_{bh}$  is the bottom-hole pressure and will be obtained from the solution of the pressure diffusivity equation without wellbore storage but including skin with the appropriate inner and outer reservoir boundary conditions. For example, we can consider a finite wellbore or line source solution for both drawdown and buildup, represented in Laplace space. So, for example, the solution  $p_{bh}$  for a fully penetrating vertical well in an composite (inner zone representing the skin zone) infinite acting reservoir will be obtained by solving the following equations:

$$\frac{1}{r} \frac{\partial}{\partial r} \left( r \frac{\partial p_s}{\partial r} \right) = \frac{1}{\eta_s} \frac{\partial p_s}{\partial t}, \quad \text{for } t > 0 \text{ and } 0 < r < r_s \quad (2.90)$$

$$\frac{1}{r} \frac{\partial}{\partial r} \left( r \frac{\partial p}{\partial r} \right) = \frac{1}{\eta} \frac{\partial p}{\partial t}, \quad \text{for } t > 0 \text{ and } r_s < r < \infty \quad (2.91)$$

Where  $\eta_s = \lambda_s / (\phi c)_s$  and  $\eta = \lambda / (\phi c)$ , and  $\lambda_s = k_s / \mu_s$  and  $\lambda = k / \mu$ .

ICs:

$$p_s(r, t = 0) = p_i = \text{constant for } 0 < r < r_s \quad (2.92)$$

$$p(r, t = 0) = p_i = \text{constant for } r_s < r < \infty \quad (2.93)$$

Continuity BCs.

$$\lambda_s \frac{\partial p_s(r=r_s, t)}{\partial r} = \lambda \frac{\partial p(r=r_s, t)}{\partial r} \quad (2.94)$$

$$p_s(r = r_s, t) = p(r = r_s, t) \quad (2.95)$$

Inner BC:

$$\left( r \frac{\partial p_s}{\partial r} \right)_{r=r_w} = [1 - H(t_p)] \frac{q_{sf}(t)B}{2\pi\lambda_s h} \quad (2.96)$$

Outer BC:

$$\lim_{r \rightarrow \infty} p(r, t) = p_i \quad (2.97)$$

The solution of the above initial-boundary-value problem will provide the solution of  $p_{bh}$  in Laplace space. It is known the solution of the above IBVP for a line-source or finite-wellbore is well-known in Laplace space. Let's derive it first for a line-source and then for a finite-wellbore here. For simplicity, delta pressures will be worked, defined by:

$$\Delta p_s(r, t) = p_i - p_s(r, t) \quad (2.98)$$

and

$$\Delta p(r, t) = p_i - p(r, t) \quad (2.99)$$

Here,  $p_i$  represents the initial pressure at the reservoir at time zero and  $z = 0$ , and for simplicity, we assume that the initial reservoir pressure and initial wellbore pressure at time zero and  $z = 0$  are identical, though this is not necessary and we can relax this assumption. Under this assumption,  $p_i = p^w(z = 0, t = 0)$ .

The pressure solutions for a composite system where the vertical well is treated as a finite-wellbore can be found in Kocak (2017).



### 3. WELLBORE HEAT FLOW MODEL EQUATIONS

#### 3.1 Derivation of Transient Wellbore Thermal Energy Equation

In this section, the starting point is the transient wellbore heat transmission equation. It seems that various forms given in papers Hasan and his coworkers and others like Spindler (2010) are quite confusing. The derivation of transient wellbore thermal energy equation is given by Hasan and Kabir (2005). Unlike them, the depth coordinate,  $z$  is chosen as positive in the upward direction.

Firstly, the energy balance equation can be written as:

$$\bar{Q} = \frac{\partial(mE)_{cv}}{\partial t} + \frac{\partial(m'E')}{\partial t} + \frac{\partial}{\partial z} \left[ w \left( H_f + \frac{1}{2} u^2 + g z \right) \right] \quad (3.1)$$

The heat received from the formation,  $Q$  can be defined by

$$Q = w c_p (T_{ei} - T_f) L_R \quad (3.2)$$

In the Eq. 3.2,  $L_R$  is the relaxation parameter. The terms  $H_f$ ,  $u$ ,  $w$ , and  $c_p$  are defined in the Nomenclature.  $T_{ei}$  depends on well depth,  $T_{ei} = T_{eiwh} - g_G z \sin \theta$ .

$$\begin{aligned} \frac{\partial}{\partial z} \left[ w \left( H_f + \frac{u^2}{2 g_c J} + \frac{g z \sin \theta}{g_c J} \right) \right] &= w \left( \frac{\partial H_f}{\partial z} + \frac{u}{g_c J} \frac{\partial u}{\partial z} - \frac{g z \sin \theta}{g_c J} \right) \\ &= w \left( c_p \frac{\partial T_f}{\partial z} - \varepsilon_{JT}^w c_p \frac{\partial p}{\partial z} + \frac{u}{g_c J} \frac{\partial u}{\partial z} - \frac{g z \sin \theta}{g_c J} \right) \end{aligned} \quad (3.3)$$

Hasan and Kabir marked that the temperature rise of the tubular material at any time may be taken to be a fraction of the increase in the fluid temperature. In this case, it can be written as:

$$m'E' = C_T x m E \quad (3.4)$$

$C_T$  in the Eq. 3.4, is the thermal storage capacity of wellbore. It is defined by

$$C_T = \frac{m'E'}{mE} \quad (3.5)$$

First and second term in the Eq. 3.1 can be written as:

$$\frac{\partial}{\partial t}(mE + m'E') = \frac{\partial}{\partial t}[mc_p T_f(1 + C_T)] \quad (3.6)$$

We can write Eq. 3.1 again

$$\begin{aligned} wc_p(T_{ei} - T_f)L_R &= \frac{\partial}{\partial t}[mc_p T_f(1 + C_T)] \\ &+ w \left( c_p \frac{\partial T_f}{\partial z} - \varepsilon_{JT}^w c_p \frac{\partial p}{\partial z} + \frac{u}{g_c J} \frac{\partial u}{\partial z} - \frac{g z \sin \theta}{g_c J} \right) \end{aligned} \quad (3.7)$$

We know that  $m = \rho A$  and  $w = \rho A u$ . The Eq. 3.7 can be given by

$$\begin{aligned} \rho A u c_p (T_{ei} - T_f)L_R &= \frac{\partial}{\partial t}[\rho A c_p T_f(1 + C_T)] \\ &+ \rho A u \left( c_p \frac{\partial T_f}{\partial z} - \varepsilon_{JT}^w c_p \frac{\partial p}{\partial z} + \frac{u}{g_c J} \frac{\partial u}{\partial z} - \frac{g z \sin \theta}{g_c J} \right) \end{aligned} \quad (3.8)$$

We assume that coefficients are constant,

$$\begin{aligned} \rho A c_p (1 + C_T) \frac{\partial T_f}{\partial t} &= \rho A u c_p L_R (T_{ei}(z) - T_f(z, t)) \\ &- \rho A u c_p \left( \frac{\partial T_f}{\partial z} - \varepsilon_{JT}^w \frac{\partial p}{\partial z} + \frac{u}{g_c c_p J} \frac{\partial u}{\partial z} - \frac{g z \sin \theta}{g_c c_p J} \right) \end{aligned} \quad (3.9)$$

We define  $\varphi$  as

$$\varphi = \varepsilon_{JT}^w \frac{\partial p}{\partial z} - \frac{u}{g_c c_p J} \frac{\partial u}{\partial z} \quad (3.10)$$

Eq. 3.8 can be written

$$\begin{aligned} \rho^w A^w c_p^w (1 + C_T) \frac{\partial T^w}{\partial t} &= \rho^w A^w u^w c_p^w L_R [T_{ei}(z) - T^w(z, t)] \\ &+ \rho^w A^w u^w c_p^w \left( \frac{\partial T^w}{\partial z} + \varphi - \frac{g \sin \theta^w}{g_c c_p^w J} \right) \end{aligned} \quad (3.11)$$

In the Eq. 3.11  $L_R$  is defined by:

$$L_R = \frac{2\pi r_{to} U_{to} \lambda_e}{\rho^w A^w u^w c_p^w [\lambda_e + r_{to} U_{to} f(t)]} \quad (3.12)$$

Let's see whether Eq. 3.11 reduces to their Alves et al. (1992) or Sagar et al. (1991) steady-state equation. For steady-state flow, Eq. 3.11 reduces to:

$$\frac{\partial T^w}{\partial z} = -L_R [T_{ei}(z) - T^w(z, t)] - \varphi + \frac{g \sin \theta^w}{g_c c_p^w J} \quad (3.13)$$

Comparing this equation with Eq. 3.14, which is repeated here,

$$\frac{\partial T^w}{\partial z} = -A(T^w - T_e) - \frac{g \sin \theta^w}{g_c c_p^w J} + \varphi \quad (3.14)$$

It looks like we have sign difference between Eqs. 3.13 and 3.14. This is expected because Eq. 3.13 considers  $z$ -axis to be positive from well-head to bottom of the well, whereas Eq. 3.14 considers  $z^w$ -axis to be positive from bottom of the well to well-head. Hence, Hasan and Kabir (1994)  $z^w = L_w - z$ . Hence,  $dz^w = -dz$  or  $dz = -dz^w$ . So, both equations are equivalent.

As we will consider  $z$  axis positive upward, then we express Eq. 3.11 in terms of the coordinate axis  $z^w$ . Hence, Eq. can be given as:

$$\begin{aligned} \rho^w A^w c_p^w (1 + C_T) \frac{\partial T^w}{\partial t} &= \rho^w A^w u^w c_p^w L_R [T_{ei}(z) - T^w(z, t)] \\ &\quad - \rho^w A^w u^w c_p^w \left( \frac{\partial T^w}{\partial z} - \varphi + \frac{g \sin \theta^w}{g_c c_p^w J} \right) \end{aligned} \quad (3.15)$$

### 3.1.1 Overall heat transfer coefficient

Sagar et al. (1991) defines  $U_t$  (which determines the heat transfer from the wellbore to the surroundings) as:

$$U_t = \frac{1}{r_{ti}} \left[ \frac{\ln(r_{ci}/r_{to})}{\lambda_{an}} + \frac{\ln(r_{wb}/r_{co})}{\lambda_{cem}} \right]^{-1} \quad (3.16)$$

where  $r_{ti}$  is the inside tubing radius,  $r_{to}$  is the outside tubing radius,  $r_{ci}$  is the inside casing radius,  $r_{wb}$  is the wellbore radius,  $\lambda_{an}$  is thermal conductivity of material in annulus, and  $\lambda_{cem}$  is thermal conductivity of cement. The units of thermal conductivity is J/m-s-K. Note that Eq. 3.16 applies if flow occurs inside a tubing placed inside a production casing.

For flow inside a production casing without a tubing, then  $U_t$  is given by (Sagar et al. 1992):

$$U_t = \frac{1}{r_{ci}} \left[ \frac{\ln(r_{wb}/r_{co})}{\lambda_{cem}} \right]^{-1} \quad (3.17)$$

### 3.1.2 Correlations for dimensionless heat transfer functions

There are various forms of equations proposed in the literature for dimensionless time function representing transient heat transfer from the wellbore to formation. For example, Hasan and Kabir (1994) proposes the following equation:

$$T_D = 1.1281\sqrt{t_D}(1 - 0.3t_D) \text{ for } 10^{-10} \leq t_D \leq 1.5 \quad (3.18)$$

and

$$T_D = (0.4063 + 0.5 \ln t_D) \left( 1 + \frac{0.3}{t_D} \right) \text{ for } t_D > 1.5 \quad (3.19)$$

Hasan and Kabir (2002) proposes the following equations:

$$T_D = \ln(e^{-0.2t_D} + (1.5 - 0.3719e^{-t_D})\sqrt{t_D}) \quad (3.20)$$

and

$$T_D = \ln[(e^{-0.2t_D} + (1.5 - 0.3719e^{-t_D})]\sqrt{t_D} \quad (3.21)$$

Cinar et al. (2006) proposes the following formula:

$$\log(T_D) = 0.007165 + 0.30947 \log(t_D) - 0.04807[\log[(t_D)]]^2 + 0.003574[\log[(t_D)]]^3 \text{ for } 10^{-2} \leq t_D \leq 10^4 \quad (3.22)$$

Kutun et al. (2015) proposes the following equation:

$$T_D = \ln(1 + 1.7\sqrt{t_D}) \quad (3.23)$$

In Eqs. 3.18-3.23,  $t_D$  represents the dimensionless time defined by

$$t_D = \frac{\alpha_t}{(r_2')^2} t \quad (3.24)$$

where  $r_2'$  is the outside radius of casing and  $\alpha_t$  is the effective/total thermal diffusivity constant of the formation.

**Table 3.1.** compares the values of  $T_D$  computed from the above equations in comparison with the rigorous solution of Carslaw and Jeager (1959) for a cylindrical wellbore.

**Table 3.1-**Comparison of Approximate and Rigorous  $T_D$  Solutions

Dimensionless time, $t_D$	Rigorous Solution (Carslaw and Jeager, 1969)	Eq. 3.17 (Hasan & Kabir, 1994)	Eq. 3.19 (Hasan & Kabir, 2002)	Eq. 3.20 (Hasan & Kabir, 2002)	Eq. 3.21 (Çınar et al. 2006)	Eq. 3.22 (Kutun et al. 2015)
$1 \times 10^{-10}$	$1.102 \times 10^{-5}$	$1.100 \times 10^{-5}$	$1.128 \times 10^{-5}$	$7.552 \times 10^{-6}$	$3.400 \times 10^{-12}$	$1.700 \times 10^{-5}$
$1 \times 10^{-6}$	$1.128 \times 10^{-3}$	$1.127 \times 10^{-3}$	$1.127 \times 10^{-3}$	$7.552 \times 10^{-4}$	$4.445 \times 10^{-5}$	$1.699 \times 10^{-3}$
$1 \times 10^{-5}$	$3.563 \times 10^{-3}$	$3.563 \times 10^{-3}$	$3.559 \times 10^{-3}$	$2.388 \times 10^{-3}$	$6.476 \times 10^{-4}$	$5.361 \times 10^{-3}$
$1 \times 10^{-4}$	$1.123 \times 10^{-2}$	$1.124 \times 10^{-2}$	$1.120 \times 10^{-3}$	$7.552 \times 10^{-3}$	$5.909 \times 10^{-3}$	$1.686 \times 10^{-2}$
$1 \times 10^{-3}$	$3.519 \times 10^{-2}$	$3.532 \times 10^{-2}$	$3.487 \times 10^{-3}$	$2.389 \times 10^{-2}$	$3.545 \times 10^{-2}$	$5.236 \times 10^{-2}$
$1 \times 10^{-2}$	0.1081	0.1094	0.1054	$7.560 \times 10^{-2}$	0.1470	0.1570
$1 \times 10^{-1}$	0.3142	0.3228	0.2987	0.2411	0.4426	0.4302
$5 \times 10^{-1}$	0.6168	0.6283	0.5911	0.5508	0.8120	0.7894
1	0.8021	0.7895	0.7802	0.7802	1.017	0.9933
1.5	0.9267	0.8738	0.9068	0.9420	1.149	1.1256
2.0	1.022	0.9784	1.001	1.063	1.248	1.2250
5.0	1.362	1.356	1.313	1.394	1.589	1.5689
10	1.651	1.651	1.585	1.555	1.871	1.8525
100	2.723	2.724	2.708	4.055	2.900	2.8904
1000	3.860	3.861	3.859	12.82	3.976	4.0029
$1 \times 10^5$	6.161	6.161	6.162	128.22	6.306	6.2889
$1 \times 10^6$	7.312	7.312	7.313	405.47	8.044	7.4390

It looks like Eq. 3.18 is the best, but Eq. 3.20 also works quite good for all dimensionless time ranges.

### 3.1.3 Earth geothermal gradient modeling

In Eq. 3.16,  $T_{ei}$  is the geothermal gradient and represent the initial condition, defined by

$$T_{ei}(z) = T_{eiwh} + (L_w - z^w) g_G \sin \theta^w \text{ for } 0 \leq z^w \leq L_w \quad (3.25)$$

Note that we can express  $T_{ei}$  in terms of the geothermal temperature gradient at depth of fluid entry as:

$$T_{ei}(z) = T_{eibh} - z^w g_G \sin \theta^w \text{ for } 0 \leq z^w \leq L_w \quad (3.26)$$

where  $T_{eiwh}$  is the initial temperature at the wellhead, and  $g_G$  is the geothermal gradient in K/m, taken as 0.03 K/m in this study.  $T_{eibh}$  represents the earth temperature at  $z = 0$  and  $t = 0$ .

## 3.2 Transient Wellbore Temperature Solutions

### 3.2.1 Specified production case-single phase oil systems

We can divide both sides of Eq. 3.15 by  $\rho^w A^w c_p^w (1 + C_T)$  to obtain:

$$\frac{\partial T^w}{\partial t} = \frac{q^w L_R}{A^w (1 + C_T)} [T_{ei}(z) - T^w(z, t)] - \frac{q^w}{A^w (1 + C_T)} \left[ \frac{\partial T^w}{\partial z} - \varphi(z^w, t) + \frac{g \sin \theta^w}{g_c c_p^w J} \right] \quad (3.27)$$

or

$$\begin{aligned} \frac{\partial T^w}{\partial t} + \frac{q^w L_R}{A^w (1 + C_T)} \frac{\partial T^w}{\partial z^w} &= \frac{q^w L_R}{A^w (1 + C_T)} [T_{ei}(z) - T^w(z, t)] \\ &+ \frac{q^w}{A^w (1 + C_T)} \left[ \varphi(z^w, t) - \frac{g \sin \theta^w}{g_c c_p^w J} \right] \end{aligned} \quad (3.28)$$

Hasan and Kabir (2005) and also Izgec et al. (2007) first solves the steady state problem by setting time derivative to zero in Eq. 3.28 to obtain:

$$\frac{\partial T_{ss}^w}{\partial z^w} = L_R [T_{ei}(z^w) - T_{ss}^w(z^w)] + \left[ \varphi(z^w, t) - \frac{g \sin \theta^w}{g_c c_p^w J} \right] \quad (3.29)$$

From the general solution of linear nonhomogenous equation,

$$\begin{aligned}
T_{SS}^w(z^w) &= T_{eihh} - g_G z^w \sin \theta^w + (T_{bh}^w - T_{eihh}) e^{-L_R z^w} \\
&+ \frac{1}{L_R} \left( g_G \sin \theta^w + \varphi - \frac{g \sin \theta^w}{g_c c_p^w J} \right) (1 - e^{-L_R z^w})
\end{aligned} \quad (3.30)$$

Now take the derivative of Eq. 3.30 with respect to  $z^w$  to obtain the gradient of wellbore temperature with respect to  $z^w$  to obtain:

$$\begin{aligned}
\frac{dT^w}{dz} &= -g_G \sin \theta^w - L_R (T_{bh}^w - T_{eihh}) e^{-L_R z^w} \\
&+ \left( g_G \sin \theta^w + \varphi - \frac{g \sin \theta^w}{g_c c_p^w J} \right) e^{-L_R z^w}
\end{aligned} \quad (3.31)$$

Recall Eq. 3.28:

$$\begin{aligned}
\frac{\partial T^w}{\partial t} + \frac{q^w L_R}{A^w (1+C_T)} \frac{\partial T^w}{\partial z^w} &= \frac{q^w L_R}{A^w (1+C_T)} [T_{ei}(z) - T^w(z, t)] \\
&+ \frac{q^w}{A^w (1+C_T)} \left[ \varphi(z^w, t) - \frac{g \sin \theta^w}{g_c c_p^w J} \right]
\end{aligned} \quad (3.32)$$

Using Eq. 3.31 in Eq. 3.32 gives:

$$\begin{aligned}
\frac{\partial T^w}{\partial t} + \frac{q^w}{A^w (1+C_T)} &\left[ -g_G \sin \theta^w - L_R (T_{bh}^w - T_{eihh}) e^{-L_R z^w} \right. \\
&\left. + \left( g_G \sin \theta^w + \varphi - \frac{g \sin \theta^w}{g_c c_p^w J} \right) e^{-L_R z^w} \right] \\
&= \frac{q^w L_R}{A^w (1+C_T)} [T_{ei}(z) - T^w(z, t)] + \frac{q^w}{A^w (1+C_T)} \left[ \varphi(z^w, t) - \frac{g \sin \theta^w}{g_c c_p^w J} \right]
\end{aligned} \quad (3.33)$$

For simplicity, we define

$$a = \frac{q^w}{A^w (1+C_T)} \quad (3.34)$$

Using Eq. 3.34 in Eq. 3.33 gives:

$$\frac{\partial T^w}{\partial t} + a \left[ -g_G \sin \theta^w - L_R (T_{bh}^w - T_{eihh}) e^{-L_R z^w} \right. \\
\left. + \left( g_G \sin \theta^w + \varphi - \frac{g \sin \theta^w}{g_c c_p^w J} \right) e^{-L_R z^w} \right]$$

$$= aL_R[T_{ei}(z) - T^w(z, t)] + aL_R \left[ \varphi(z^w, t) - \frac{g \sin \theta^w}{g_c c_p^w J} \right] \quad (3.35)$$

Eq. 3.35 can be rearranged as:

$$\begin{aligned} \frac{\partial T^w}{\partial t} + aL_R T^w(z^w, t) &= aL_R T_{ei}(z^w) + a \left[ \varphi - \frac{g \sin \theta^w}{g_c c_p^w J} \right] + a g_G \sin \theta^w \\ &+ aL_R (T_{bh}^w - T_{eih}) e^{-L_R z^w} - a \left( g_G \sin \theta^w + \varphi - \frac{g \sin \theta^w}{g_c c_p^w J} \right) e^{-L_R z^w} \end{aligned} \quad (3.36)$$

Let's define

$$P(t) = aL_R \quad (3.37)$$

and

$$\begin{aligned} Q(t) &= aL_R T_{ei}(z^w) + a \left( \varphi - \frac{g \sin \theta^w}{g_c c_p^w J} \right) + a g_G \sin \theta^w \\ &+ aL_R (T_{bh}^w - T_{eih}) e^{-L_R z^w} - a \left( g_G \sin \theta^w + \varphi - \frac{g \sin \theta^w}{g_c c_p^w J} \right) e^{-L_R z^w} \end{aligned} \quad (3.38)$$

Note that  $Q(t) = Q = \text{constant}$  is actually independent of time,  $t$ . Then, Eq. 3.38 can be written as:

$$\frac{\partial T^w}{\partial t} + P(t) T^w(z^w, t) = Q(t) \quad (3.39)$$

We solve this first order, nonhomogeneous ODE subject to the initial condition given by:

$$T^w(z^w, t = 0) = T_{ei}(z^w) \quad (3.40)$$

The general solution of Eq. 3.40 is given by

$$T^w(z^w, t) = e^{-\int a_{LR} dt} \left[ \int e^{\int a_{LR} dt} Q(t) dt + B \right] \quad (3.41)$$

or

$$T^w(z^w, t) = e^{-a_{LR}t} \int e^{a_{LR}t} Q(t) dt + e^{-a_{LR}t} B \quad (3.42)$$

The integral in the RHS of Eq. 3.42 can be performed as follows:

$$\int e^{a_{LR}t} Q(t) dt = Q \int e^{a_{LR}t} dt = \frac{Q}{a_{LR}} e^{a_{LR}t} \quad (3.43)$$

Using Eq. 3.43 in Eq. 3.42 gives:

$$T^w(z^w, t) = e^{-a_{LR}t} \frac{Q}{a_{LR}} e^{a_{LR}t} + e^{-a_{LR}t} B = \frac{Q}{a_{LR}} + e^{-a_{LR}t} B \quad (3.44)$$

To determine B, we use the initial condition given by Eq. 3.40. So, the constant B can be determined as:

$$T^w(z^w, t = 0) = \frac{Q}{a_{LR}} + e^{-a_{LR} \cdot 0} B = T_{ei}(z^w) \Rightarrow B = T_{ei}(z^w) - \frac{Q}{a_{LR}} \quad (3.45)$$

Using B given by Eq. 3.45 in Eq. 3.44 gives the wellbore temperature as a function of  $z^w$  and  $t$  as:

$$\begin{aligned} T^w(z^w, t) &= \frac{Q}{a_{LR}} + e^{-a_{LR}t} \left( T_{ei}(z^w) - \frac{Q}{a_{LR}} \right) \\ &= e^{-a_{LR}t} T_{ei}(z^w) + \frac{Q}{a_{LR}} (1 - e^{-a_{LR}t}) \end{aligned} \quad (3.46)$$

Using  $Q$  given by Eq. 3.38 in Eq. 3.46 gives:

$$\begin{aligned} T^w(z^w, t) &= e^{-a_{LR}t} T_{ei}(z^w) + \frac{Q}{a_{LR}} (1 - e^{-a_{LR}t}) \\ &= e^{-a_{LR}t} T_{ei}(z^w) + \frac{(1 - e^{-a_{LR}t})}{a_{LR}} x \end{aligned}$$

$$\left[ \begin{array}{l} aL_R T_{ei}(z^w) + a \left( \varphi - \frac{g \sin \theta^w}{g_c c_p^w J} \right) + a g_G \sin \theta^w L_R \\ + aL_R (T_{bh}^w - T_{eih}) e^{-L_R z^w} \\ - \left( g_G \sin \theta^w + \varphi - \frac{g \sin \theta^w}{g_c c_p^w J} \right) e^{-L_R z^w} \end{array} \right] \quad (3.47)$$

Defining

$$\psi = g_G \sin \theta^w + \varphi - \frac{g \sin \theta^w}{g_c c_p^w J} \quad (3.48)$$

Eq. 3.47 can be written as:

$$\begin{aligned} T^w(z^w, t) &= e^{-aL_R t} T_{ei}(z^w) + \\ &\frac{(1-e^{-aL_R t})}{aL_R} \left[ \begin{array}{l} aL_R T_{ei}(z^w) + a \left( \varphi - \frac{g \sin \theta^w}{g_c c_p^w J} \right) + a g_G \sin \theta^w + aL_R (T_{bh}^w - T_{eih}) e^{-L_R z^w} \\ - a\psi e^{-L_R z^w} \end{array} \right] \\ &= e^{-aL_R t} T_{ei}(z^w) + T_{ei}(z^w) + \frac{1}{L_R} \left( \varphi - \frac{g \sin \theta^w}{g_c c_p^w J} \right) + \frac{1}{L_R} g_G \sin \theta^w \\ &\quad + (T_{bh}^w - T_{eih}) e^{-L_R z^w} - \frac{1}{L_R} \psi e^{-L_R z^w} - e^{-aL_R t} T_{ei}(z^w) \\ &\quad - \frac{e^{-aL_R t}}{L_R} \left( \varphi - \frac{g \sin \theta^w}{g_c c_p^w J} \right) \\ &\quad - \frac{e^{-aL_R t}}{L_R} g_G \sin \theta^w - (T_{bh}^w - T_{eih}) e^{-L_R t} e^{-L_R z^w} + \frac{e^{-aL_R t}}{L_R} \psi e^{-L_R z^w} \end{aligned} \quad (3.49)$$

Cancelling  $e^{-aL_R t}$  term

$$\begin{aligned} T^w(z^w, t) &= T_{ei}(z^w) + \frac{(1-e^{-aL_R t})}{L_R} \left( \varphi - \frac{g \sin \theta^w}{g_c c_p^w J} \right) + \frac{(1-e^{-aL_R t})}{L_R} g_G \sin \theta^w \\ &\quad - \frac{(1-e^{-aL_R t})}{L_R} \psi e^{-L_R z^w} + (T_{bh}^w - T_{eih})(1 - e^{-aL_R t}) e^{-L_R z^w} \end{aligned} \quad (3.50)$$

Bracketing common term as  $\frac{(1-e^{-aL_R t})}{L_R}$

$$\begin{aligned} T^w(z^w, t) &= T_{ei}(z^w) + \frac{(1-e^{-aL_R t})}{L_R} \left( g_G \sin \theta^w + \varphi - \frac{g \sin \theta^w}{g_c c_p^w J} \right) + \\ &\quad \frac{(1-e^{-aL_R t})}{L_R} \psi e^{-L_R z^w} + (T_{bh}^w - T_{eih})(1 - e^{-aL_R t}) e^{-L_R z^w} \end{aligned} \quad (3.51)$$

Because  $\psi = g_G \sin \theta^w + \varphi - \frac{g \sin \theta^w}{g_c c_p^w J}$ , Eq. 3.51 result in

$$T^w(z^w, t) = T_{ei}(z^w) + \frac{(1-e^{-aL_R t})}{L_R} \psi - \frac{(1-e^{-aL_R t})}{L_R} \psi e^{-L_R z^w} + (1 - e^{-aL_R t})(T_{bh}^w - T_{eih})e^{-L_R z^w} \quad (3.52)$$

$$T^w(z^w, t) = T_{ei}(z^w) + \frac{(1 - e^{-aL_R t})(1 - e^{-L_R z^w})}{L_R} \psi + (T_{bh}^w - T_{eih})(1 - e^{-aL_R t})e^{-L_R z^w} \quad (3.53)$$

### 3.2.2 Buildup case for-single phase oil systems

Here, we follow Hasan et al. (2005). As in drawdown, they assume that rate variation with well depth becomes negligible quickly. With wellhead shut-in,  $q^w = 0$ , and the relaxation distance for buildup becomes:

$$L'_R = \rho^w A^w u^w L_R = \begin{cases} \frac{2\pi}{c_p^w} \left[ \frac{r_{ti} U_t \lambda_e}{\lambda_e + f(t) r_{ti} U_t} \right] & \text{for } L_R = \frac{2\pi}{c_p^w (\rho^w A^w u^w)} \left[ \frac{r_{ti} U_t \lambda_e}{\lambda_e + f(t) r_{ti} U_t} \right] \\ \frac{2\pi}{c_p^w} \left[ \frac{r_{ci} U_t \lambda_e}{\lambda_e + f(t) r_{ci} U_t} \right] & \text{for } L_R = \frac{2\pi}{c_p^w (\rho^w A^w u^w)} \left[ \frac{r_{ci} U_t \lambda_e}{\lambda_e + f(t) r_{ci} U_t} \right] \end{cases} \quad (3.54)$$

Then transient wellbore temperature equation for this case becomes:

$$\frac{dT^w}{d\Delta t} = \frac{L'_R}{\rho^w A^w (1+C_T)} [T_{ei}(z^w) - T^w(z^w, \Delta t)] \quad (3.55)$$

or can be rearranged as:

$$\frac{dT^w}{d\Delta t} + \frac{L'_R}{\rho^w A^w (1+C_T)} T^w(z^w, \Delta t) = \frac{L'_R}{\rho^w A^w (1+C_T)} T_{ei}(z^w) \quad (3.56)$$

where the earth temperature  $T_{ei}$  is given by Eq. 3.25,

$$T_{ei}(z^w) = T_{eih} - z^w g_G \sin \theta^w \text{ for } 0 \leq z^w \leq L_w \quad (3.57)$$

In Eq. 3.55 or 3.56,  $\Delta t$  is the elapsed time during buildup, i.e.,  $\Delta t = t - t_p$ , where  $t$  is the total time. Eq. 3.56 is a first order linear nonhomogeneous equation. We solve it subject to an initial condition given by:

$$T^w(z^w, \Delta t = 0) = T_{fo}(z^w) \quad (3.58)$$

where  $T_{fo}$  is the fluid temperature at the moment of shut-in.

The solution of Eq. 3.56 is given by:

$$T^w(z^w, \Delta t) = e^{-\int a' d\Delta t'} [e^{\int a' d\Delta t'} Q(\Delta t') d\Delta t' + B] \quad (3.59)$$

or

$$T^w(z^w, \Delta t) = e^{a'\Delta t} \int e^{-a'\Delta t'} Q(\Delta t') d\Delta t' + e^{-a'\Delta t} B \quad (3.60)$$

Where

$$a' = \frac{L'_R}{\rho^w A^w (1 + C_T)} \quad (3.61)$$

and

$$Q = \frac{L'_R}{\rho^w A^w (1 + C_T)} T_{ei}(z^w) = dT_{ei}(z^w) \quad (3.61)$$

The integral in the RHS of Eq. 3.60 can be performed as follows:

$$\int e^{a'\Delta t'} Q(\Delta t') d\Delta t' = Q \int e^{a'\Delta t'} d\Delta t' = \frac{Q}{a'} e^{a'\Delta t'} = T_{ei}(z^w) e^{a'\Delta t'} \quad (3.62)$$

Using Eq. 3.63 in Eq. 3.60 gives:

$$T^w(z^w, \Delta t) = e^{a'\Delta t} T_{ei}(z^w) e^{a'\Delta t'} + e^{-a'\Delta t} B = T_{ei}(z^w) + B e^{a'\Delta t} \quad (3.63)$$

To find the constant  $B$ , we use the initial condition given by Eq. 3.58. Doing so, we determine  $B$  as:

$$T^w(z^w, \Delta t = 0) = T_{ei}(z^w) + B e^{a'0} \Rightarrow T_{ei}(z^w) + B = T_{fo}(z^w) \quad (3.64)$$

or

$$B = [T_{fo}(z^w) - T_{ei}(z^w)] \quad (3.65)$$

Using Eq. 3.66 in Eq. 3.65 gives the solution for the buildup:

$$T^w(z^w, \Delta t) = T_{ei}(z^w) + [T_{fo}(z^w) - T_{ei}(z^w)] e^{a'\Delta t} \quad (3.66)$$

It looks like the analytical equation given by Eq. 3.54 and its solution given by Eq. 3.66 ignores the temperature gradient in the  $z$ -direction.

We'll start with Eq. 3.15,

$$\begin{aligned} \rho^w A^w c_p^w (1 + C_T) \frac{\partial T^w}{\partial t} &= \rho^w A^w u^w c_p^w L_R [T_{ei}(z) - T^w(z^w, t)] \\ &\quad - \rho^w A^w u^w c_p^w \left( \frac{\partial T^w}{\partial z} - \varphi(z^w, t) + \frac{g \sin \theta^w}{g_c c_p^w J} \right) \end{aligned} \quad (3.67)$$

And express it using Eq. 3.12 in Eq. 3.15 as:

$$\begin{aligned} \rho^w A^w c_p^w (1 + C_T) \frac{\partial T^w}{\partial t} &= c_p^w \frac{2\pi r_{to} U_{to} \lambda_e}{c_p^w [\lambda_e + r_{to} U_{to} f(t)]} [T_{ei}(z) - T^w(z^w, t)] \\ &\quad - \rho^w q^w c_p^w \left( \frac{\partial T^w}{\partial z} - \varphi(z^w, t) + \frac{g \sin \theta^w}{g_c c_p^w J} \right) \end{aligned} \quad (3.68)$$

Now, we use the definition of  $L'_R$  given by Eq. 3.54 in Eq. 3.69 to obtain:

$$\begin{aligned} \rho^w A^w c_p^w (1 + C_T) \frac{\partial T^w}{\partial t} &= c_p^w L'_R [T_{ei}(z) - T^w(z^w, t)] \\ &\quad - \rho^w q^w c_p^w \left( \frac{\partial T^w}{\partial z} - \varphi(z^w, t) + \frac{g \sin \theta^w}{g_c c_p^w J} \right) \end{aligned} \quad (3.69)$$

For buildup period;  $t = t_p + \Delta t$ , where  $t_p$  is the producing time, and hence we can define Eq. 3.69 in terms of  $\Delta t$  as:

$$\begin{aligned} \rho^w A^w c_p^w (1 + C_T) \frac{\partial T^w}{\partial \Delta t} &= c_p^w L'_R [T_{ei}(z) - T^w(z^w, \Delta t)] \\ -\rho^w q^w c_p^w \left( \frac{\partial T^w}{\partial z} - \varphi(z^w, \Delta t) + \frac{g \sin \theta^w}{g_c c_p^w J} \right) & \end{aligned} \quad (3.70)$$

We can divide both sides of Eq. 3.70 by  $\rho^w A^w c_p^w (1 + C_T)$  to obtain:

$$\begin{aligned} \frac{\partial T^w}{\partial \Delta t} &= \frac{L'_R}{\rho^w A^w (1 + C_T)} [T_{ei}(z) - T^w(z^w, \Delta t)] \\ -\frac{q^w}{A^w (1 + C_T)} \left[ \frac{\partial T^w}{\partial z} - \varphi(z^w, \Delta t) + \frac{g \sin \theta^w}{g_c c_p^w J} \right] & \end{aligned} \quad (3.71)$$

or

$$\begin{aligned} \frac{\partial T^w}{\partial \Delta t} + \frac{q^w}{A^w (1 + C_T)} \frac{\partial T^w}{\partial z} &= \frac{L'_R}{\rho^w A^w (1 + C_T)} [T_{ei}(z) - T^w(z^w, \Delta t)] \\ + \frac{q^w}{A^w (1 + C_T)} \left[ \varphi(z^w, \Delta t) - \frac{g \sin \theta^w}{g_c c_p^w J} \right] & \end{aligned} \quad (3.72)$$

Hasan and Kabir (2005) and also Izgec et al. (2009) first solves the steady state problem by setting time derivative to zero in Eq. 3.72, and the following equation is obtained:

$$\begin{aligned} T_{SS}^w(z^w) &= T_{eibh} - z^w g_G \sin \theta^w + (T_{bh} - T_{eibh}) e^{-\frac{L'_R z^w}{\rho^w q^w}} \\ + \frac{1}{\left( \frac{L'_R}{\rho^w q^w} \right)} \left( g_G \sin \theta^w + \varphi - \frac{g \sin \theta^w}{g_c c_p^w J} \right) \left( 1 - e^{-\frac{L'_R z^w}{\rho^w q^w}} \right) & \end{aligned} \quad (3.73)$$

Now take the derivative of Eq. 3.73 with respect to  $z^w$  to obtain the gradient of wellbore temperature with respect to  $z^w$  to obtain:

$$\begin{aligned} \frac{dT^w}{dz} &= -g_G \sin \theta^w - \left( \frac{L'_R}{\rho^w q^w} \right) (T_{bh} - T_{eih}) e^{-\frac{L'_R z^w}{\rho^w q^w}} \\ &+ \left( g_G \sin \theta^w + \varphi - \frac{g \sin \theta^w}{g_c c_p^w J} \right) \left( 1 - e^{-\frac{L'_R z^w}{\rho^w q^w}} \right) \end{aligned} \quad (3.74)$$

Recall Eq. 3.72:

$$\begin{aligned} \frac{\partial T^w}{\partial \Delta t} + \frac{q^w}{A^w(1+C_T)} \frac{\partial T^w}{\partial z} &= \frac{L'_R}{\rho^w A^w(1+C_T)} [T_{ei}(z) - T^w(z^w, \Delta t)] \\ &+ \frac{q^w}{A^w(1+C_T)} \left[ \varphi(z^w, \Delta t) - \frac{g \sin \theta^w}{g_c c_p^w J} \right] \end{aligned} \quad (3.75)$$

Using Eq. 3.74 in Eq. 3.75 gives:

$$\begin{aligned} \frac{\partial T^w}{\partial \Delta t} + \frac{q^w}{A^w(1+C_T)} &\left[ -g_G \sin \theta^w - \left( \frac{L'_R}{\rho^w q^w} \right) (T_{bh} - T_{eih}) e^{-\frac{L'_R z^w}{\rho^w q^w}} \right. \\ &\left. + \left( g_G \sin \theta^w + \varphi - \frac{g \sin \theta^w}{g_c c_p^w J} \right) \left( 1 - e^{-\frac{L'_R z^w}{\rho^w q^w}} \right) \right] \\ &= \frac{L'_R}{\rho^w A^w(1+C_T)} [T_{ei}(z) - T^w(z^w, \Delta t)] + \frac{q^w}{A^w(1+C_T)} \left[ \varphi(z^w, \Delta t) - \frac{g \sin \theta^w}{g_c c_p^w J} \right] \end{aligned} \quad (3.76)$$

For simplicity, we define

$$a = \frac{q^w}{A^w(1+C_T)} \quad (3.77)$$

Using Eq. 3.77 in Eq. 3.76 gives:

$$\begin{aligned} \frac{\partial T^w}{\partial \Delta t} + a &\left[ -g_G \sin \theta^w - \left( \frac{L'_R}{\rho^w q^w} \right) (T_{bh} - T_{eih}) e^{-\frac{L'_R z^w}{\rho^w q^w}} \right. \\ &\left. + \left( g_G \sin \theta^w + \varphi - \frac{g \sin \theta^w}{g_c c_p^w J} \right) \left( 1 - e^{-\frac{L'_R z^w}{\rho^w q^w}} \right) \right] \\ &= a \left( \frac{L'_R}{\rho^w q^w} \right) [T_{ei}(z) - T^w(z^w, \Delta t)] + a \left[ \varphi(z^w, \Delta t) - \frac{g \sin \theta^w}{g_c c_p^w J} \right] \end{aligned} \quad (3.78)$$

Eq. 3.78 can be rearranged as:

$$\frac{\partial T^w}{\partial \Delta t} + a \left( \frac{L'_R}{\rho^w q^w} \right) T^w(z^w, \Delta t) = a \left( \frac{L'_R}{\rho^w q^w} \right) T_{ei}(z) + a \left( \varphi(z^w, \Delta t) - \frac{g \sin \theta^w}{g_c c_p^w J} \right)$$

$$\begin{aligned}
& + a g_G \sin \theta^w + a \left( \frac{L'_R}{\rho^w q^w} \right) (T_{bh} - T_{eih}) e^{-\frac{L'_R z^w}{\rho^w q^w}} \\
& - a \left( g_G \sin \theta^w + \varphi - \frac{g \sin \theta^w}{g_c c_p^w J} \right) e^{-\frac{L'_R z^w}{\rho^w q^w}} \quad (3.79)
\end{aligned}$$

Let's define

$$P(\Delta t) = a \left( \frac{L'_R}{\rho^w q^w} \right) \quad (3.80)$$

and

$$\begin{aligned}
Q(\Delta t) &= a \left( \frac{L'_R}{\rho^w q^w} \right) T_{ei}(z^w) + a \left( \varphi - \frac{g \sin \theta^w}{g_c c_p^w J} \right) + a g_G \sin \theta^w \\
& + a \left( \frac{L'_R}{\rho^w q^w} \right) (T_{bh} - T_{eih}) e^{-\frac{L'_R z^w}{\rho^w q^w}} - a \left( g_G \sin \theta^w + \varphi - \frac{g \sin \theta^w}{g_c c_p^w J} \right) e^{-\frac{L'_R z^w}{\rho^w q^w}} \quad (3.81)
\end{aligned}$$

Then, Eq. 3.79 can be written as:

$$\frac{dT^w}{d\Delta t} + P(\Delta t) T^w(z^w, \Delta t) = Q(\Delta t) \quad (3.82)$$

We solve Eq. 3.82 subject to an initial condition given by:

$$T^w(z^w, \Delta t = 0) = T_{fo}(z^w) \quad (3.83)$$

where  $T_{fo}$  is the fluid temperature at the moment of shut-in.

The general solution of Eq. 3.82 is given by

$$T^w(z^w, \Delta t) = e^{-a \left( \frac{L'_R}{\rho^w q^w} \right) \Delta t} \int e^{a \left( \frac{L'_R}{\rho^w q^w} \right) \Delta t} Q(t) dt + e^{-a \left( \frac{L'_R}{\rho^w q^w} \right) \Delta t} B \quad (3.84)$$

The integral in the RHS of Eq. 3.84 can be performed as follows:

$$\int e^{a \left( \frac{L'_R}{\rho^w q^w} \right) \Delta t} Q(t) dt = Q \int e^{a \left( \frac{L'_R}{\rho^w q^w} \right) \Delta t} dt = \frac{Q}{a \left( \frac{L'_R}{\rho^w q^w} \right)} e^{a \left( \frac{L'_R}{\rho^w q^w} \right) \Delta t} \quad (3.85)$$

Using Eq. 3.85 in Eq. 3.84 gives:

$$\begin{aligned}
T^w(z^w, \Delta t) &= e^{-a\left(\frac{L'_R}{\rho^w q^w}\right)\Delta t} \frac{Q}{a\left(\frac{L'_R}{\rho^w q^w}\right)} e^{a\left(\frac{L'_R}{\rho^w q^w}\right)\Delta t} + e^{-a\left(\frac{L'_R}{\rho^w q^w}\right)\Delta t} B \\
&= \frac{Q}{a\left(\frac{L'_R}{\rho^w q^w}\right)} + e^{-a\left(\frac{L'_R}{\rho^w q^w}\right)\Delta t} B
\end{aligned} \tag{3.86}$$

To determine B, we use the initial condition given by Eq. 3.82. So, the constant B can be determined as:

$$\begin{aligned}
T^w(z^w, \Delta t = 0) &= \frac{Q}{a\left(\frac{L'_R}{\rho^w q^w}\right)} + e^{-a\left(\frac{L'_R}{\rho^w q^w}\right)\Delta t} B = T_{fo}(z^w) \\
\Rightarrow B &= T_{fo}(z^w) - \frac{Q}{a\left(\frac{L'_R}{\rho^w q^w}\right)}
\end{aligned} \tag{3.87}$$

Using B given by Eq. 3.87 gives the wellbore temperature as a function of  $z^w$  and  $t$  as:

$$\begin{aligned}
T^w(z^w, \Delta t) &= \frac{Q}{a\left(\frac{L'_R}{\rho^w q^w}\right)} + e^{-a\left(\frac{L'_R}{\rho^w q^w}\right)\Delta t} \left( T_{fo}(z^w) - \frac{Q}{a\left(\frac{L'_R}{\rho^w q^w}\right)} \right) \\
&= e^{-a\left(\frac{L'_R}{\rho^w q^w}\right)\Delta t} T_{fo}(z^w) + \frac{Q}{a\left(\frac{L'_R}{\rho^w q^w}\right)} \left[ 1 - e^{-a\left(\frac{L'_R}{\rho^w q^w}\right)\Delta t} \right]
\end{aligned} \tag{3.88}$$

Using  $Q$  given by Eq. 3.81 in 3.88 gives:

$$\begin{aligned}
T^w(z^w, \Delta t) &= e^{-a\left(\frac{L'_R}{\rho^w q^w}\right)\Delta t} T_{fo}(z^w) + \frac{\left( 1 - e^{-a\left(\frac{L'_R}{\rho^w q^w}\right)\Delta t} \right)}{a\left(\frac{L'_R}{\rho^w q^w}\right)} x \\
&\left[ \begin{aligned}
&a\left(\frac{L'_R}{\rho^w q^w}\right) T_{ei}(z^w) + a\left(\varphi - \frac{g \sin \theta^w}{g_c c_p^w J}\right) + a g_G \sin \theta^w \\
&+ a\left(\frac{L'_R}{\rho^w q^w}\right) (T_{bh} - T_{eih}) e^{-\frac{L'_R z^w}{\rho^w q^w}} \\
&- a\left(g_G \sin \theta^w + \varphi - \frac{g \sin \theta^w}{g_c c_p^w J}\right) e^{-\frac{L'_R z^w}{\rho^w q^w}}
\end{aligned} \right]
\end{aligned} \tag{3.89}$$

Defining

$$\psi = g_G \sin \theta^w + \varphi - \frac{g \sin \theta^w}{g_c c_p^w J} \quad (3.90)$$

Eq. 3.89 can be written as:

$$\begin{aligned} T^w(z^w, \Delta t) &= e^{-a(L_R)\Delta t} T_{fo}(z^w) + (1 - e^{-a(L_R)\Delta t}) T_{ei}(z^w) \\ &+ [T_{bh}(\Delta T) - T_{eihh}] (1 - e^{-a(L_R)\Delta t}) e^{-L_R z} \\ &+ \frac{(1 - e^{-a(L_R)\Delta t})(1 - e^{-L_R z})}{L_R} \psi(z, t) \end{aligned} \quad (3.91)$$

### 3.3 Steady-State Wellbore Temperature Solutions

#### 3.3.1 Specified production case-single phase oil systems

The steady-state wellbore temperature equation is derived from transient wellbore temperature equation in section 3.2.1. If we let time  $t$  goes to infinity in the Eq. 3.52, Eq. 3.52 reduces to the steady-state temperature which is denoted by  $T_{ss}^w$  given by:

$$T_{ss}^w(z) = T_{ei}(z^w) + \frac{(1 - e^{-L_R z})}{L_R} \psi + [T_{bh} - T_{eihh}] e^{-L_R z} \quad (3.92)$$

which is similar to the equation derived by Alves et al. (1992) and Hasan and Kabir (1994). The momentum equation may be approximated for single-phase flow liquid under incompressible fluid assumption as (Hasan and Kabir, 2002):

$$\frac{1}{\rho^w} \frac{\partial p^w}{\partial z} \approx g \sin \theta^w \quad (3.93)$$

The acceleration term in Eq. 3.9 can be ignored as compared to the pressure gradient term;

$$\varphi = \varepsilon_{JT}^w \frac{\partial p^w}{\partial z} \quad (3.94)$$

The J-T coefficient for liquids may be approximated as:

$$\varepsilon_{JT}^w = (\rho^w g_c c_p^w J)^{-1} \quad (3.95)$$

Using Eq. 3.93 and 3.95 in Eq. 3.94 gives:

$$\varphi = \left( \rho^w g_c c_p^w J \right)^{-1} \left( \rho^w g \sin \theta^w \right) = \frac{g \sin \theta^w}{g_c c_p^w J} \quad (3.96)$$

Then Eq. 3.90 under these assumptions reduces to:

$$\psi = g_G \sin \theta^w \quad (3.97)$$

### 3.3.2 Buildup case for single-phase oil systems

We recall Eq. 3.91 which is transient wellbore temperature equation for buildup:

$$\begin{aligned} T^w(z^w, \Delta t) = & e^{-a(L_R)\Delta t} T_{fo}(z^w) + (1 - e^{-a(L_R)\Delta t}) T_{ei}(z^w) \\ & + [T_{bh}(\Delta T) - T_{eihh}] (1 - e^{-a(L_R)\Delta t}) e^{-L_R z} \\ & + \frac{(1 - e^{-a(L_R)\Delta t})(1 - e^{-L_R z})}{L_R} \psi(z, t) \end{aligned} \quad (3.98)$$

If we let shut-in time  $\Delta t$  and  $L_R$  goes to infinity in Eq. 3.98, Eq. 3.98 reduces to the steady-state temperature equation, given by

$$T_{SS}^w(z^w) = \lim_{\Delta t \rightarrow \infty} T^w(z^w, \Delta t) = T_{ei}(z^w) = T_{eihh} - z^w g_G \sin \theta^w \quad (3.99)$$

which is the geothermal gradient equation, as expected.



#### 4. COUPLING WITH TRANSIENT SANDFACE/BOTTOMHOLE PRESSURE AND TEMPERATURE SOLUTIONS

To compute transient wellbore pressure and temperature solutions, we use the equations derived in Kocak's MS thesis (2017).

##### 4.1 Transient Bottomhole Pressure

For this model,  $q_{sf}$  can be computed from following Eq. (4.1) derived by Kocak (2017);

$$\bar{q}_{sf}(s) = \frac{\bar{q}_{wh}(s)}{[1+C_s\Psi(s)]} \quad (4.1)$$

where  $\Psi(s)$  is given in Kocak's Thesis.

$p_{bh}$  is computed from:

$$\bar{p}_{bh}(s) = \frac{p^w(z=0,t=0)}{s} - \frac{\bar{q}_{wh}(s)B_o\Psi(s)}{[1+C_s\Psi(s)]} \text{ for } 0 < r < r_s \quad (4.2)$$

For a wellbore including momentum balance,  $\bar{q}^w(z, s)$  and  $\bar{p}^w(z, s)$  in terms of the known inputs are  $\bar{q}_{wh}$  and  $\bar{p}_{bh}$  can be represented by a system of equations, which can be written in a matrix-vector form as:

$$\begin{bmatrix} \bar{q}^w(z, s) \\ \bar{p}^w(z, s) \end{bmatrix} = T_{wr}(z, s) \begin{bmatrix} \bar{q}_{wh}(s) \\ \bar{p}_{bh}(s) \end{bmatrix} + \begin{bmatrix} \bar{q}_{int}^w \\ \bar{p}_{int}^w \end{bmatrix} \quad (4.3)$$

Where the matrix  $T_{wr}(z, s)$  is a 2x2 matrix given by:

$$T_{wr}(z, s) = \begin{bmatrix} \cosh \zeta z & -\frac{A^w c^w}{\zeta} (\sin \zeta z - \tanh \zeta L_w \cosh \zeta z) \\ \frac{\zeta}{A^w c^w} \sinh \zeta z & (\cosh \zeta z + \tanh \zeta L_w \sinh \zeta z) \end{bmatrix} \quad (4.4)$$

and  $\bar{q}_{int}^w$  and  $\bar{p}_{int}^w$  are given by, respectively,

$$\bar{q}_{int}^w = \frac{A^w c^w}{\zeta} \frac{p^w(z=0,t=0)}{s} (\sin \zeta z - \tanh \zeta L_w \cosh \zeta z) \quad (4.5)$$

and

$$\bar{p}_{int}^w = \frac{p^w(z,t=0)}{s} - \frac{p^w(z=0,t=0)}{s} (\cosh \zeta z + \tanh \zeta L_w \sinh \zeta z) \quad (4.6)$$

In Eqs. 4.4-4.6,  $\zeta$  defined by

$$\zeta = \sqrt{\rho^w c^w (s^2 + R_s)} \quad (4.7)$$

It follows from Eqs. 4.3-4.7 that  $\bar{q}^w(z, s)$  and  $\bar{p}^w(z, s)$  can be expressed, respectively, as:

$$\begin{aligned} \bar{q}^w(z, s) = & \cosh \zeta z \bar{q}_{wh}(s) - \frac{A^w c^w}{\zeta} (\sin \zeta z - \tanh \zeta L_w \cosh \zeta z) \bar{p}_{bh}(s) + \\ & \frac{A^w c^w}{\zeta} \frac{p^w(z=0,t=0)}{s} (\sin \zeta z - \tanh \zeta L_w \cosh \zeta z) \end{aligned} \quad (4.8)$$

and

$$\begin{aligned} \bar{p}^w(z, s) = & \frac{s}{A^w c^w} \sinh \zeta z \bar{q}_{wh}(s) + (\cosh \zeta z + \tanh \zeta L_w \sinh \zeta z) \bar{p}_{bh}(s) + \\ & \frac{p^w(z,t=0)}{s} - \frac{p^w(z=0,t=0)}{s} (\cosh \zeta z + \tanh \zeta L_w \sinh \zeta z) \end{aligned} \quad (4.9)$$

Evaluating  $\bar{q}^w(z, s)$  at  $z = 0$  so that we can have an expression for the sandface volumetric rate  $\bar{q}_{sf}(s)$  as:

$$\begin{aligned} \bar{q}_{sf}(s) = & \cosh \zeta 0 \bar{q}_{wh}(s) - \frac{A^w c^w}{\zeta} (\sin \zeta 0 - \tanh \zeta L_w \cosh \zeta 0) \bar{p}_{bh}(s) + \\ & \frac{A^w c^w}{\zeta} \frac{p^w(z=0,t=0)}{s} (\sin \zeta 0 - \tanh \zeta L_w \cosh \zeta 0) \end{aligned} \quad (4.10)$$

Eq. 4.10 can be simplified as:

$$\bar{q}_{sf}(s) = \bar{q}_{wh}(s) + \frac{A^w c^w}{\zeta} \tanh \zeta L_w \bar{p}_{bh}(s) - \frac{A^w c^w}{\zeta} \frac{p^w(z=0,t=0)}{s} \tanh \zeta L_w \quad (4.11)$$

Now using Eq. 4.2 in Eq. 4.11 gives:

$$\begin{aligned} \bar{q}_{sf}(s) = & \bar{q}_{wh}(s) + \frac{A^w c^w}{\zeta} \tanh \zeta L_w \left\{ \frac{p^w(z=0,t=0)}{s} - \frac{\bar{q}_{wh}(s) B_o \Psi(s)}{[1 + C_s \Psi(s)]} \right\} - \\ & \frac{A^w c^w}{\zeta} \frac{p^w(z=0,t=0)}{s} \tanh \zeta L_w \end{aligned} \quad (4.12)$$

Or can be simplified as:

$$\bar{q}_{sf}(s) = \bar{q}_{wh}(s) - \frac{A^w c^w B_o}{\zeta} \tanh \zeta L_w B_o \Psi(s) \bar{q}_{sf} \quad (4.13)$$

which can be rearranged to solve  $\bar{q}_{sf}(s)$  as:

$$\bar{q}_{sf}(s) = \frac{\bar{q}_{wh}(s)}{\left[1 + \frac{A^w c^w B_o}{\zeta} \tanh \zeta L_w B_o \Psi(s)\right]} \quad (4.14)$$

So, this provides us to compute  $q_{sf}$  is defined by following equation from wellhead flow rate:

$$q_{sf}(t) = q_{bh}(t) = L^{-1} \left\{ \frac{\bar{q}_{wh}(s)}{\cosh \zeta L_w \left[1 + \frac{u A^w c^w}{\zeta} \tanh \zeta L_w \Psi(r_w, s)\right]} \right\} \quad (4.15)$$

where

$$\zeta = \sqrt{\rho^w c^w (s^2 + R s)} \quad (4.16)$$

We can compute the bottomhole pressure  $p_{bh}$  as a function of  $t$  by numerically inverting the following Laplace space solution,

$$p_{bh}(t) = p^w(z=0, t) = p^w(z=0, t=0) - L^{-1} \left\{ \frac{\Psi(r_w, s) \bar{q}_{wh}(s)}{\cosh \zeta L_w \left[1 + \frac{u A^w c^w}{\zeta} \tanh \zeta L_w \Psi(r_w, s)\right]} \right\} \quad (4.17)$$

## 4.2 Transient Wellbore Pressure Distribution Solution

Now let's express Eq. 4.9 in terms of the sandface rate  $\bar{q}_{sf}(s)$  by replacing the bottom-hole  $\bar{p}_{bh}(s)$  in Eq. 4.9 by Eq. 4.2. Doing so gives:

$$\begin{aligned} \bar{p}^w(z, s) = & \frac{\zeta}{A^w c^w} \sinh \zeta z \bar{q}_{wh}(s) + (\cosh \zeta z + \\ & \tanh \zeta L_w \sinh \zeta z) \left[ \frac{p^w(z=0, t=0)}{s} - B_o \Psi(s) \bar{q}_{sf} \right] + \frac{p^w(z, t=0)}{s} - \frac{p^w(z=0, t=0)}{s} (\cosh \zeta z + \\ & \tanh \zeta L_w \sinh \zeta z) \end{aligned} \quad (4.18)$$

or can be simplified as:

$$\begin{aligned} \bar{p}^w(z, s) = & \frac{p^w(z, t=0)}{s} + \frac{\zeta}{A^w c^w} \sinh \zeta z \bar{q}_{wh}(s) \\ & - (\cosh \zeta z + \tanh \zeta L_w \sinh \zeta z) B_o \Psi(s) \bar{q}_{sf} \end{aligned} \quad (4.19)$$

Eq. 4.19 can be used to compute wellbore pressure profile as a function of  $z$  because both well head and sandface flow rates are specified in the RHS of Eq. 4.19.

The wellbore pressure  $p^w$  as a function of  $z$  and  $t$  can be computed by numerically inverting the following Laplace space solutions,

$$p^w(z, t) = p^w(z, t = 0) - L^{-1} \left\{ \frac{\frac{\zeta}{sA^w c^w} \frac{\sinh \zeta z}{\cosh \zeta L_w} \bar{q}_{wh}(s)}{+ \frac{(\cosh \zeta z + \tanh \zeta L_w \sinh \zeta z) \Psi(r_w, s)}{\cosh \zeta L_w \left[ 1 + \frac{sA^w c^w}{\zeta} \tanh \zeta L_w \Psi(r_w, s) \right]}} \bar{q}_{wh}(s) \right\} \quad (4.20)$$

The initial wellbore pressure distribution is computed from the hydraulic gradient of the fluid:

$$p^w(z, t = 0) = p_{bh}(t = 0) - \frac{\rho^w g}{g_c} z \quad (4.21)$$

where  $\rho^w$  is the density of fluid evaluated and treated as constant evaluated at initial bottomhole pressure and temperature,  $g$  ( $= 9.80665 \frac{m}{s^2}$ ) is the gravity acceleration, and  $g_c$  is the unit conversion factor and equal to  $1 \text{ kg-m/kgf-s}^2$

Note that  $p_{bh}(t = 0) = p^w(z = 0, t = 0)$ .

### 4.3 Transient Wellbore Flow Rate Distribution Solution

Similarly, we can compute the flow rate profile as a function of  $z$  from Eq. 4.8. For convenience, we express Eq. 4.8 in terms of the sandface rate  $\bar{q}_{sf}(s)$  by replacing the bottom-hole  $\bar{p}_{bh}(s)$  in Eq. 4.8 by Eq. 4.2. Doing so gives:

$$\bar{q}^w(z, s) = \cosh \zeta z \bar{q}_{wh}(s) - \frac{A^w c^w}{\zeta} (\sin \zeta z - \tanh \zeta L_w \cosh \zeta z) \left[ \frac{p^w(z=0, t=0)}{s} - B_o \Psi(s) \bar{q}_{sf} \right] + \frac{A^w c^w}{\zeta} \frac{p^w(z=0, t=0)}{s} (\sin \zeta z - \tanh \zeta L_w \cosh \zeta z) \quad (4.22)$$

Or simplifying gives:

$$\bar{q}^w(z, s) = \cosh \zeta z \bar{q}_{wh}(s) + \frac{A^w c^w B_o}{\zeta} (\sinh \zeta z - \tanh \zeta L_w \cosh \zeta z) \Psi(s) \bar{q}_{sf} \quad (4.23)$$

The wellbore flow rate  $q^w$  as a function of  $z$  and  $t$  can be computed by numerically inverting the following Laplace space solution,

$$q^w(z, t) = L^{-1} \left\{ \frac{\cosh \zeta z}{\cosh \zeta L_w} - \frac{sA^w c^w}{\zeta} \frac{(\tanh \zeta L_w \cosh \zeta z - \sinh \zeta z) \Psi(r_w, s)}{\cosh \zeta L_w \left[ 1 + \frac{sA^w c^w}{\zeta} \tanh \zeta L_w \Psi(r_w, s) \right]} \bar{q}_{wh}(s) \right\} \quad (4.24)$$

#### 4.4 Numerical Inversion of Solutions

We present the results for skin zero case, and compare the accuracy of the Stehfest (Stehfest 1970) and Crump (Crump 1976) inversion algorithms, as per Onur et al. (2017).

In Figure 2 and Figure 3, we can show the results for drawdown and buildup period, respectively. These results were obtained with both Stehfest and Crump algorithms. We used a value of 12 as the Stehfest parameter ( $N_{stef} = 12$ ). In the Crump algorithm, we used a value  $10^{-6}$  as the error tolerance.

In Figure 2 and Figure 3, we show the effect of the skin on the drawdown sandface solutions computed from both the conventional WBS model by using the Stehfest algorithm and the momentum model by using the Crump algorithm. As shown in these figures, oscillations at early times in the sandface flow rate reduces as the skin factor reduces. In all cases, the momentum effects finish at 0.01 hour; thus, all solutions for the momentum model are obtained with Crump algorithm.

The all results are generated with the synthetic test data in Table 4.1.

**Table 4.1:** Well, wellbore and earth physical and thermal property input data

Property	Value	Property	Value
$\lambda_e$ [J/m-s-K]	1.731	$r_{ci}$ [m]	0.0968
$\lambda_{cem}$ [J/m-s-K]	0.346	$r_{co}$ [m]	0.1095
$\alpha_e$ [m/s]	$7.3806 \times 10^{-7}$	$R_c$ [dimensionless]	$6.13576 \times 10^3$
$g_G$ [K/m]	0.03	$\delta/D$ [dimensionless]	$5.0 \times 10^{-4}$
$g$ [m/s <sup>2</sup> ]	9.80665	$f$ [dimensionless]	0.035
$C_T$ [dimensionless]	0	$R$ [s <sup>-1</sup> ]	$1.01153 \times 10^{-2}$
$L_w$ [m]	1550	$C$ [m <sup>3</sup> /Pa]	$4.91795 \times 10^{-8}$
$\theta^w$ [°]	90	$T_{eih}$ [K]	291.48
$q_{wh}$ [m <sup>3</sup> /s]	$3.29799 \times 10^{-3}$	$T_{eibh}$ [K]	351.48
		$\gamma^w$ [Pa/m]	$8.18424 \times 10^3$

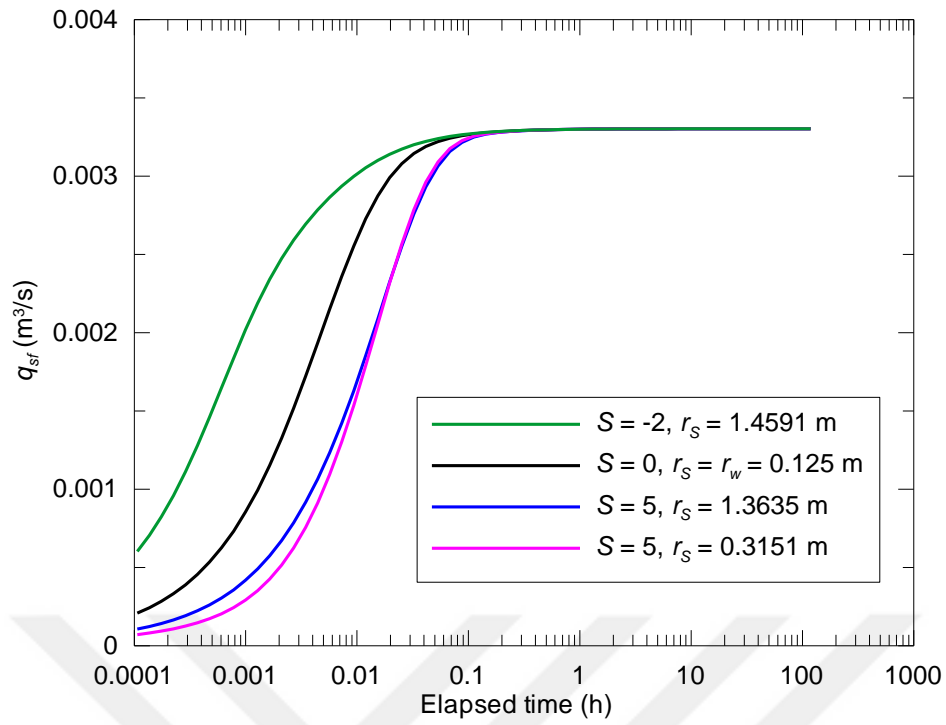


**Figure 4.1:** Effect of skin-zone properties on sandface flow rates computed from the WBS model for drawdown.

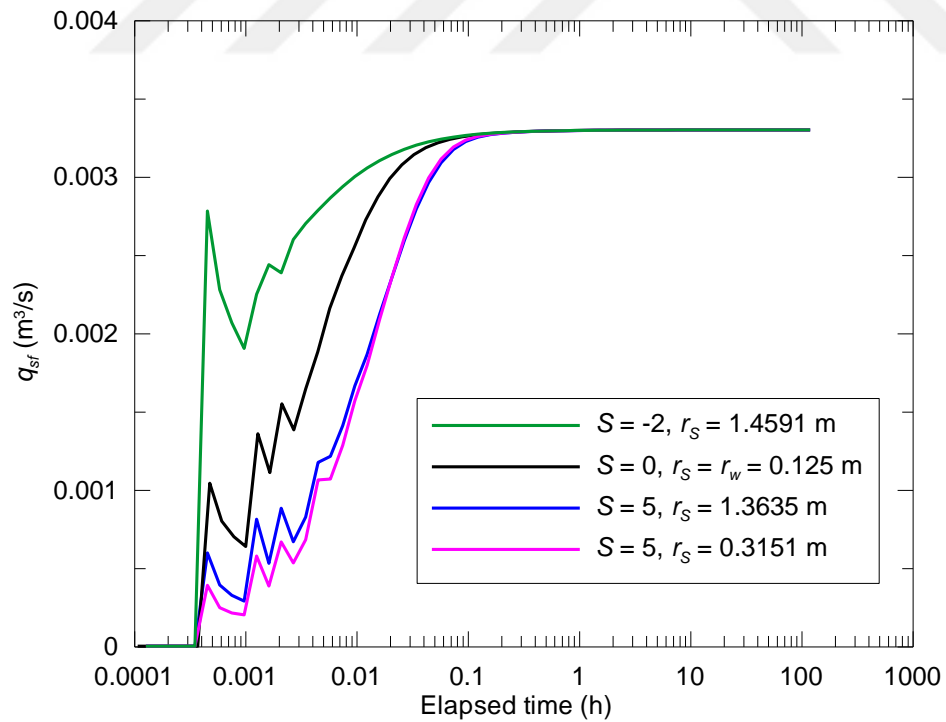


**Figure 4.2:** Effect of skin-zone properties on sandface flow rates computed from the momentum model for drawdown.

## 5. SANDFACE AND WELLBORE PRESSURE, FLOW RATE AND TEMPERATURE BEHAVIORS

In this section, we investigate the behaviors of sandface and wellbore flow rate, pressure, and temperature distributions. All results are generated with the data in Table 4.1. In additional Table 4.1, the data is used in Table 5.1 and 5.2.

**Table 5.1:** Simulation input data used for verification example (Onur and Cinar, 2016)

Reservoir and Fluid Properties				Component Physical and Thermal Properties			
$k$ [m <sup>2</sup> ]	$1.056 \times 10^{-13}$	$B_o$ [m <sup>3</sup> /sm <sup>3</sup> ]	1.05427	Property	Oil	Water	Solid Matrix
$\phi$ [fraction]	0.29	$B_w$ [m <sup>3</sup> /sm <sup>3</sup> ]	1.022	$\rho$ [kg/m <sup>3</sup> ]	834.56	1000.03	2643.05
$h$ [m]	30.48	$c_o$ [Pa <sup>-1</sup> ]	$1.077 \times 10^{-9}$	$c_p$ [J/kg-K]	2177.1	4186.8	962.96
$T^0$ [K]	351.48	$c_w$ [Pa <sup>-1</sup> ]	$4.398 \times 10^{-10}$	$\beta$ [K <sup>-1</sup> ]	$7.2 \times 10^{-4}$	$9.0 \times 10^{-4}$	$9.0 \times 10^{-5}$
$p^0$ [MPa]	13.06	$\mu_o$ [Pa.s]	$2.949 \times 10^{-3}$	$\epsilon_{JT}$ [K/Pa]	$-4.432 \times 10^{-7}$	$-1.933 \times 10^{-7}$	n/a
$p_b$ [MPa]	2.758	MW <sub>o</sub> [kg/gmol]	0.321	$\varphi$ [K/Pa]	$1.072 \times 10^{-7}$	$4.554 \times 10^{-8}$	n/a
$r_{wb}$ [m]	0.125	$T_c$ [K]	585	$c_{pR}$ [unitless]	0.7456	1.7182	
$r_e$ [m]	15000	$p_c$ [MPa]	1.2551	$\lambda_t$ [J/m-s-K]	3.4615	for saturated porous medium	
$S$ [unitless]	variable	$\omega$ , Acentric Factor	0.9196	$\alpha_t$ [m <sup>2</sup> /s]	$1.420 \times 10^{-6}$	for saturated porous medium	
$s_w$ [fraction]	0.15	$\eta_o$ [m <sup>2</sup> /s]	$8.717 \times 10^{-3}$	$(\rho c_p)_t$ [J/m <sup>3</sup> -K]	$2.437 \times 10^6$	for saturated porous medium	
$c_r$ [Pa <sup>-1</sup> ]	$4.351 \times 10^{-10}$	CPG1 [J/g-K]	14.108	$(\rho c_p \varphi)$ [J/m <sup>3</sup> -Pa]	$5.630 \times 10^{-2}$	for fluid	
$c_t$ [Pa <sup>-1</sup> ]	$1.417 \times 10^{-9}$	CPG2 [J/g-K]	1.8223	$\varphi^*_{t_i}$ [K/Pa]	$2.310 \times 10^{-8}$	for saturated porous medium	

**Table 5.2:** Skin zone parameters for verification example (Onur and Cinar, 2016)

	Skin factor, $S$ [unitless]	$k$ [m <sup>2</sup> ]	$k_s$ [m <sup>2</sup> ]	$r_s$ [m]
Case 1	-2	$1.0560 \times 10^{-13}$	$5.6748 \times 10^{-13}$	1.4591
Case 2	5	$1.0560 \times 10^{-13}$	$3.4148 \times 10^{-14}$	1.3635
Case 3	5	$1.0560 \times 10^{-13}$	$1.6842 \times 10^{-14}$	0.3151

### 5.1 Sandface Flow Rate Behavior for Production and Buildup Cases

In this section, our results are obtained for sandface flow rate behavior with the conventional WBS and the momentum models. As seen in Onur et al. (2016), the sandface flow rate is input to the semi-analytical temperature model. Also, this input ( $q_{sf}$ ) determines the sandface or bottomhole temperature behaviors.

In this section, we observe sandface flow rate behavior with elapsed time in the Figure 4 and 5 for drawdown and buildup for zero skin case, respectively.

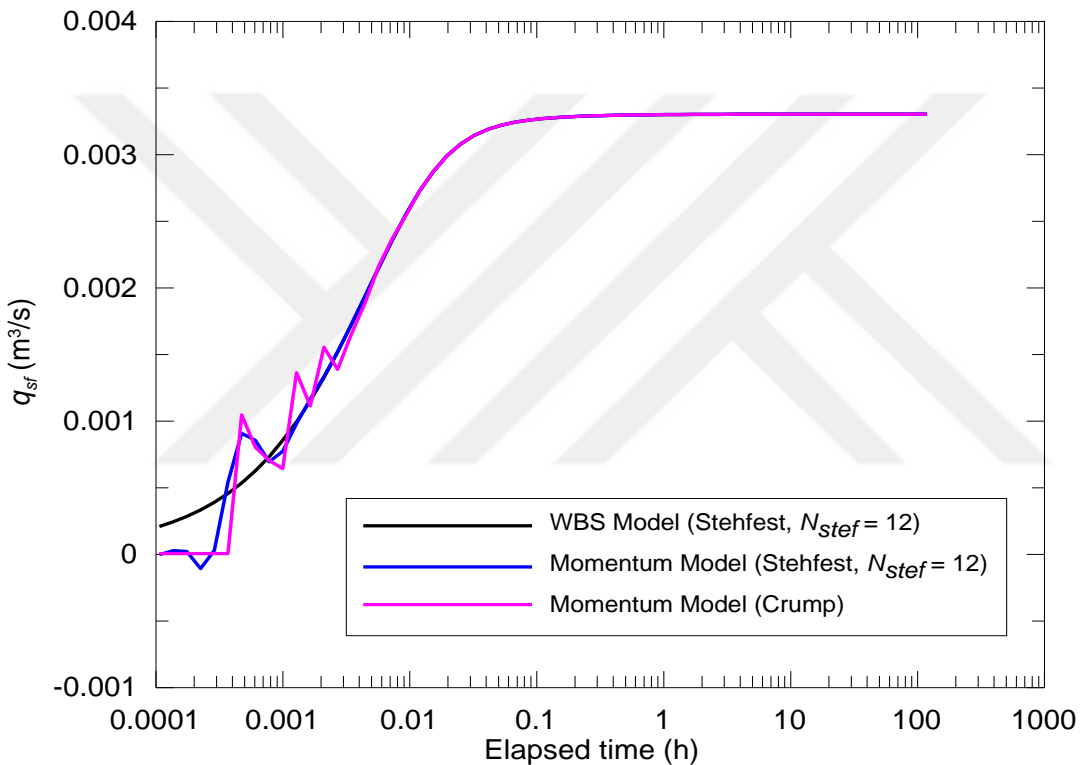


**Figure 5.1:** Comparison of sandface flow rates inverted by the Stehfest and Crump algorithms for the WBS and momentum models for drawdown; skin zero case.

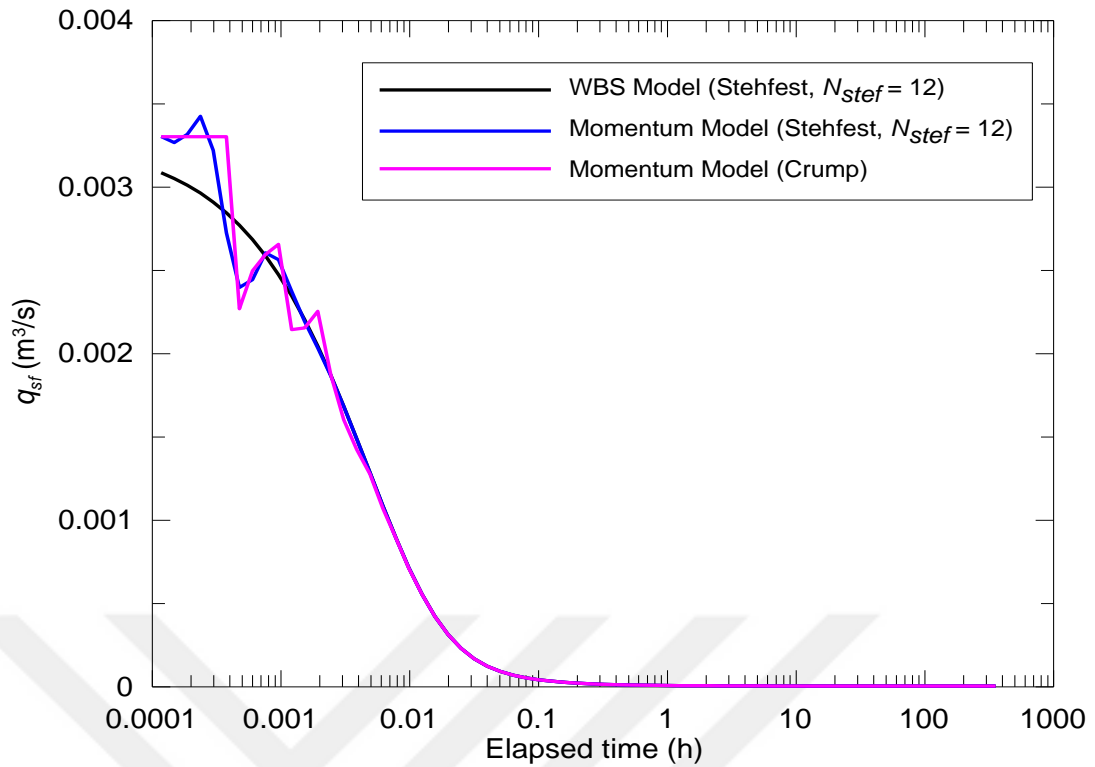


**Figure 5.2:** Comparison of sandface flow rates inverted by the Stehfest and Crump algorithms for the WBS and momentum models for buildup; skin zero case.

We can not see any oscillations in the WBS model for both drawdown and buildup periods. Unlike WBS, we observe oscillations at early time in the momentum model. These oscillations are owing to pressure waves in the well.

## 5.2 Flow Rate and Pressure Distributions along the Wellbore for Production and Buildup Cases

Here, we observe the transient wellbore pressure and flow rate behaviors, and their gradients.

We can see a cartesian plot of the transient wellbore pressure and wellbore length in Figure 6, and a cartesian plot of the flow rate and wellbore length in Figure 7. Also, Figure 8 and 9 shows gradients of the wellbore pressure and the flow rate. These figures are obtained for zero skin case for drawdown period. In these figures, the well length  $z$  is from 0 to 500 m. Our goal is to examine the gauge location on transient temperature responses. The transient wellbore pressure,  $p^w$  decreases linearly with slope, as expected for a slightly compressible fluid., and its gradient  $dp^w/dz$  shows

small changes in the slope of Figure 11. As shown in the Figure 8 and 9, the flow rate  $q^w$  approaches to the wellhead flow rate and its gradient  $dq^w/dz$  approaches zero uniformly, as producing time increases. The wellbore flow rate increases linearly with time at late times, but not linear at early times.

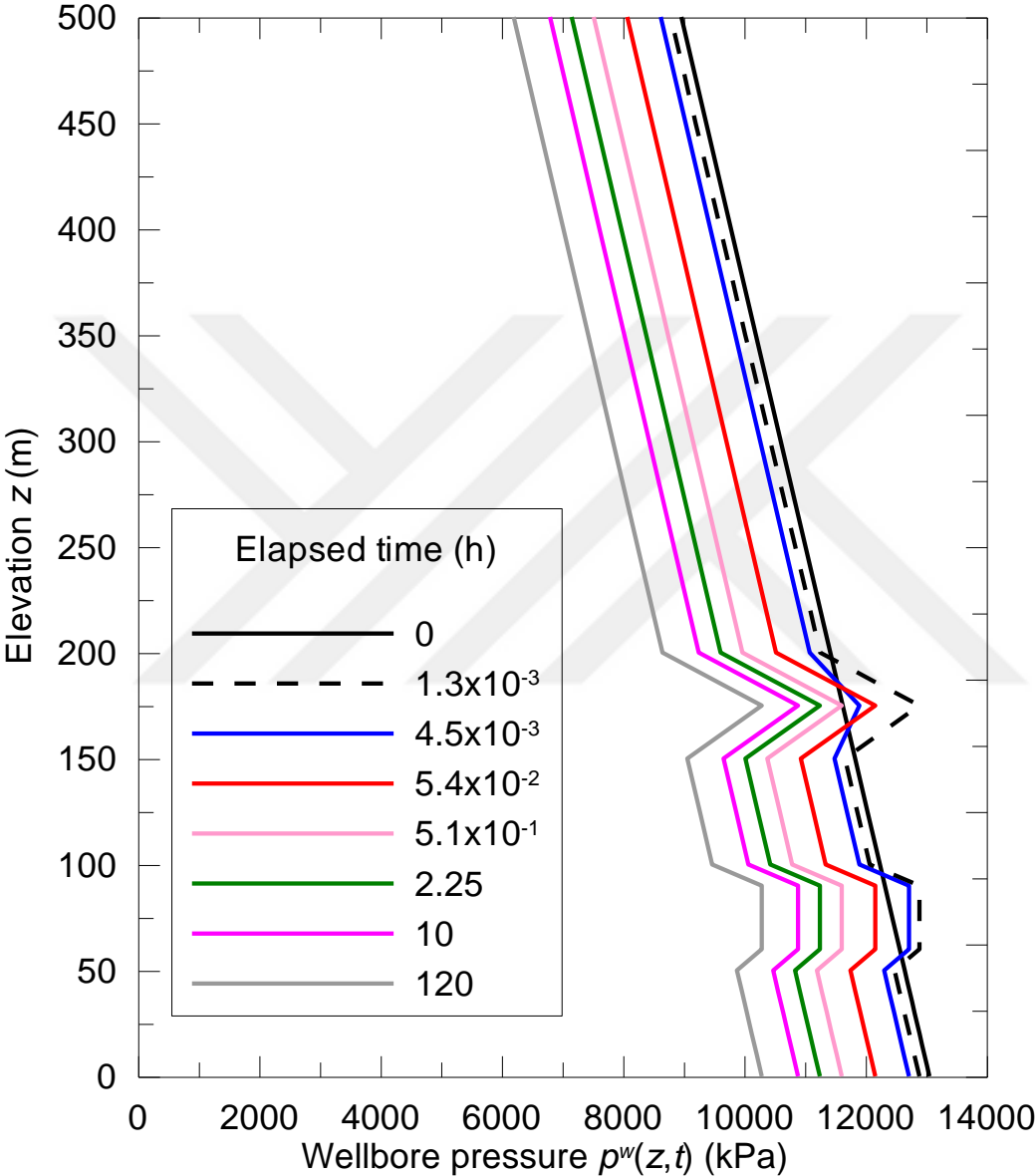


**Figure 5.3:**  $z$  vs  $p^w$  plot at various drawdown times, momentum model, zero skin case.

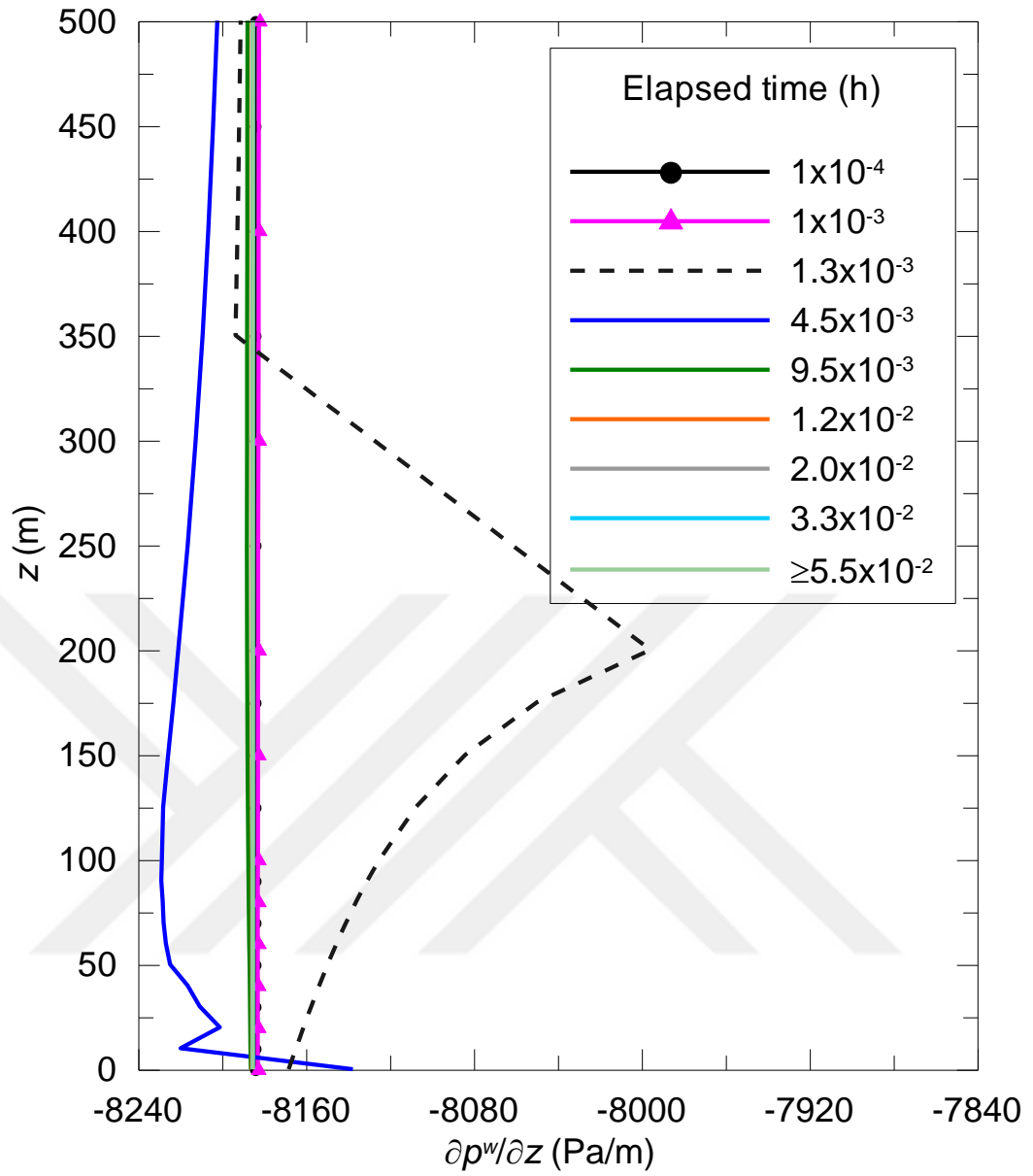


**Figure 5.4:**  $z$  vs  $dp^w/dz$  plot at various drawdown times, momentum model, zero skin case.

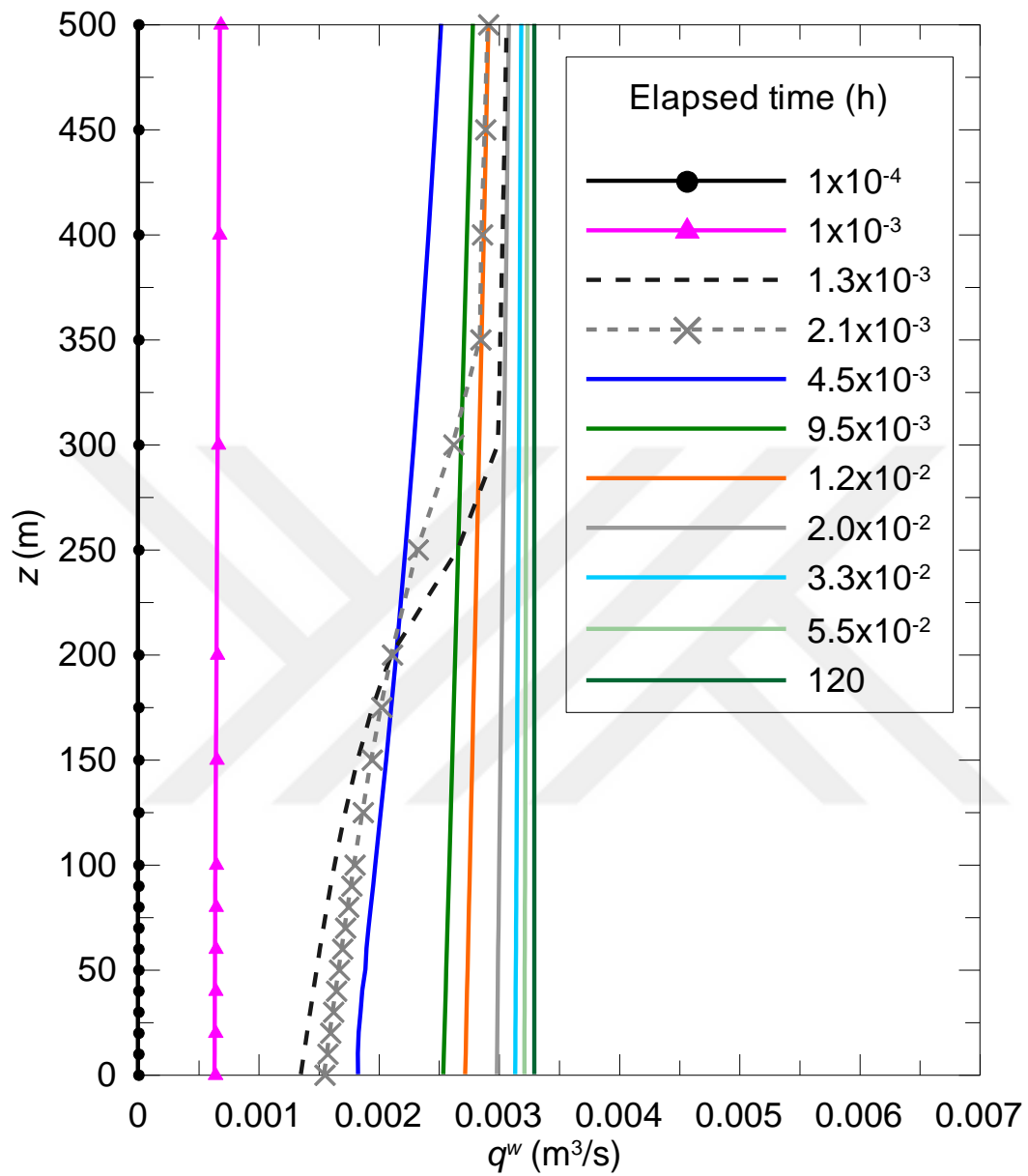


**Figure 5.5:**  $z$  vs  $q^w$  plot at various drawdown times, momentum model, zero skin case.

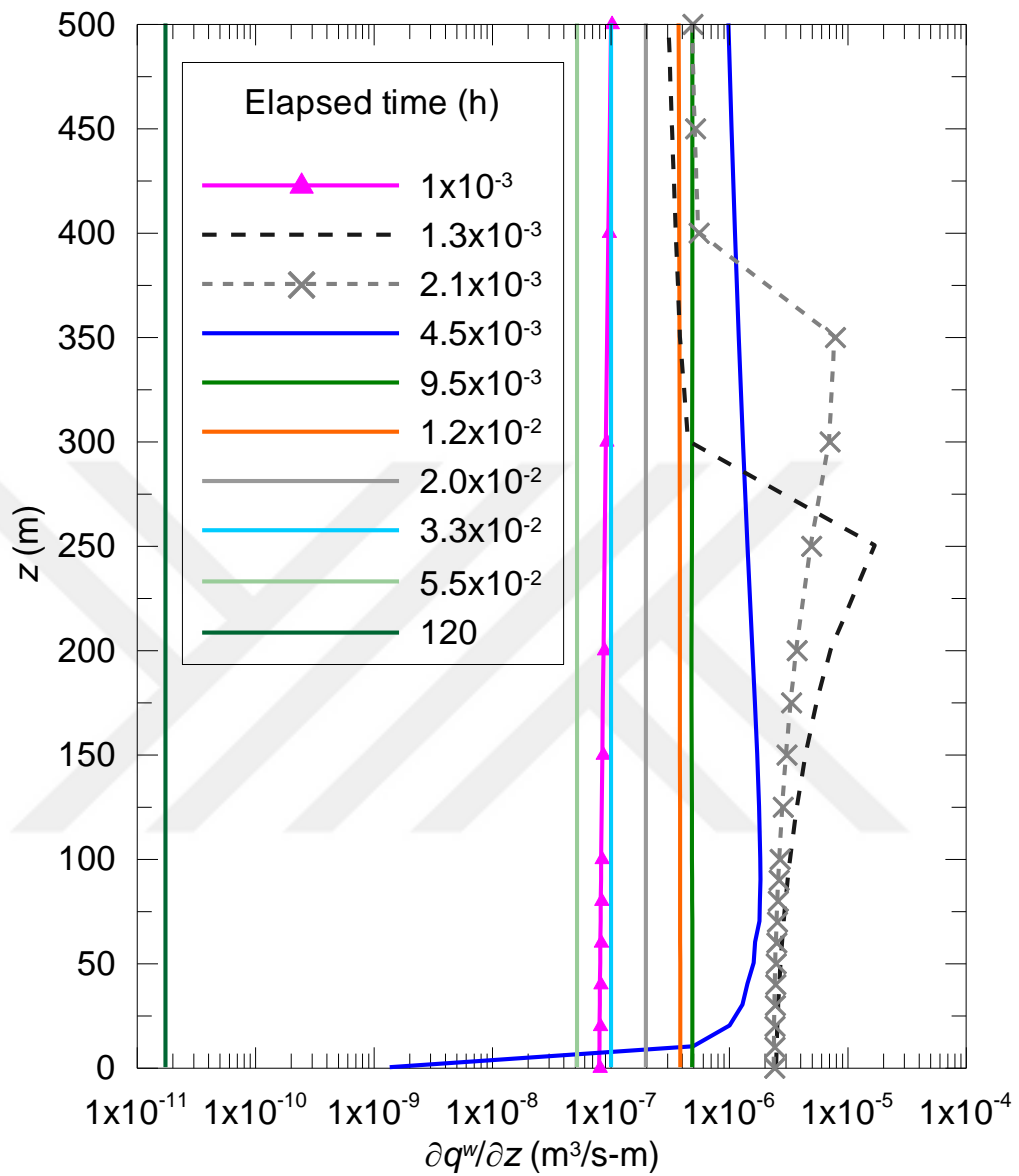


**Figure 5.6:**  $z$  vs  $dq_w/dz$  plot at various drawdown times, momentum model, zero skin case.

In the Figure 10 and 11, we can see the cartesian plots of the transient wellbore flow rate and pressure gradient for buildup. Because the gradient of the flow rate is negative, its absolute values are plotted in Figure 11. Unlike drawdown period, the wellbore flow rate decreases, and the wellbore pressure increases along the wellbore in buildup. In Figure 12, we can see the effect of skin zone on the flow rate at various elapsed drawdown times. The negative skin increases the wellbore flow rate, whereas positive skin reduces the wellbore flow rate.

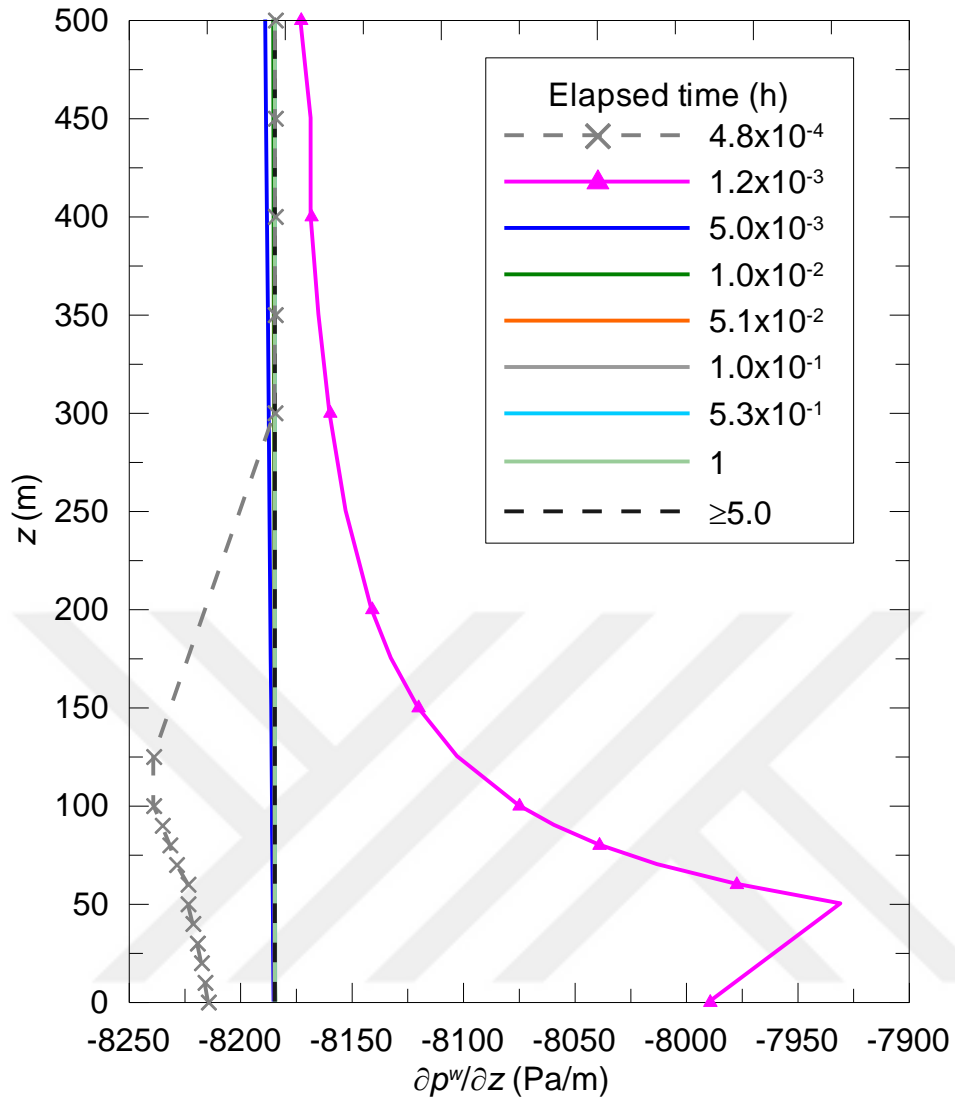
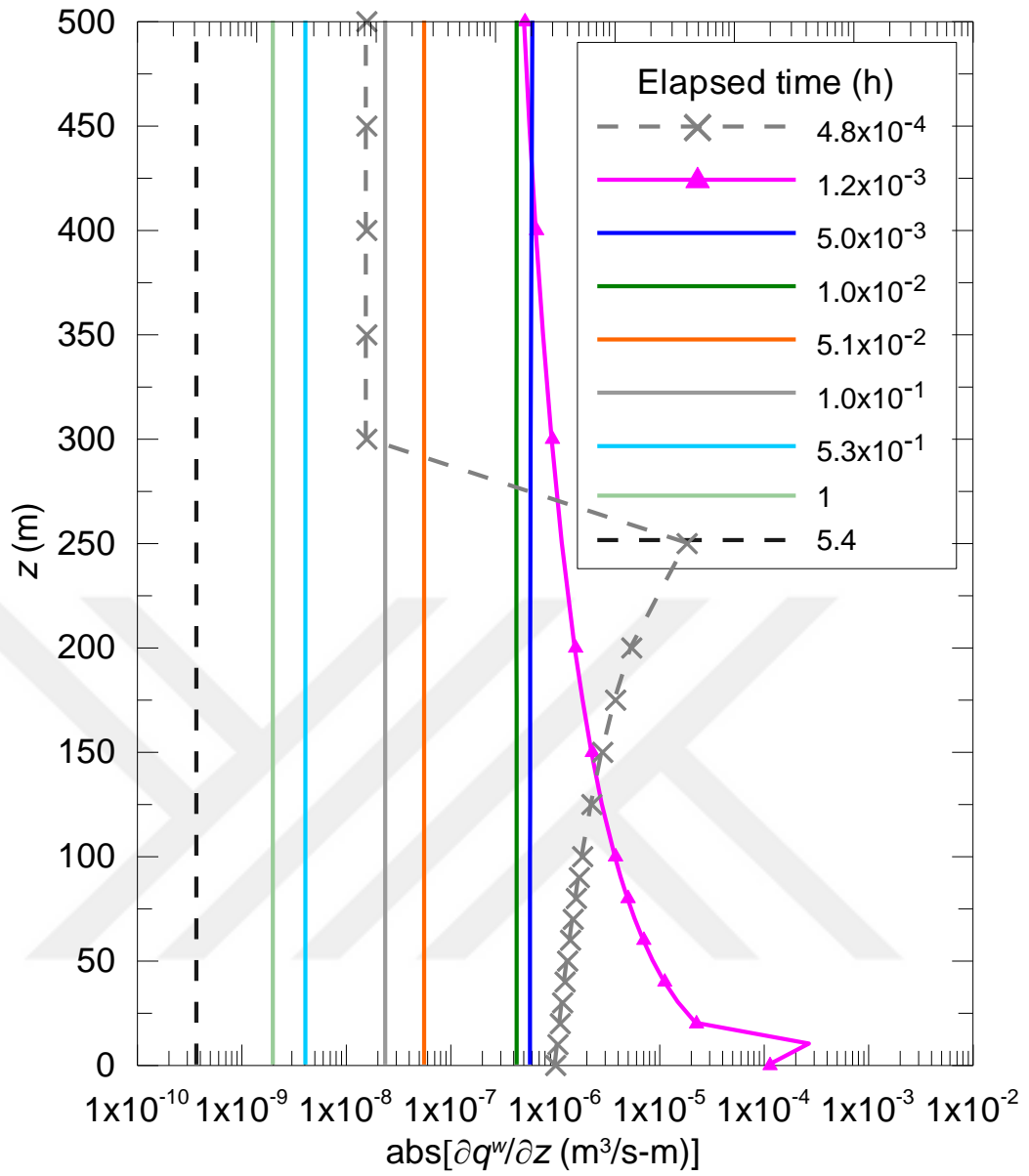
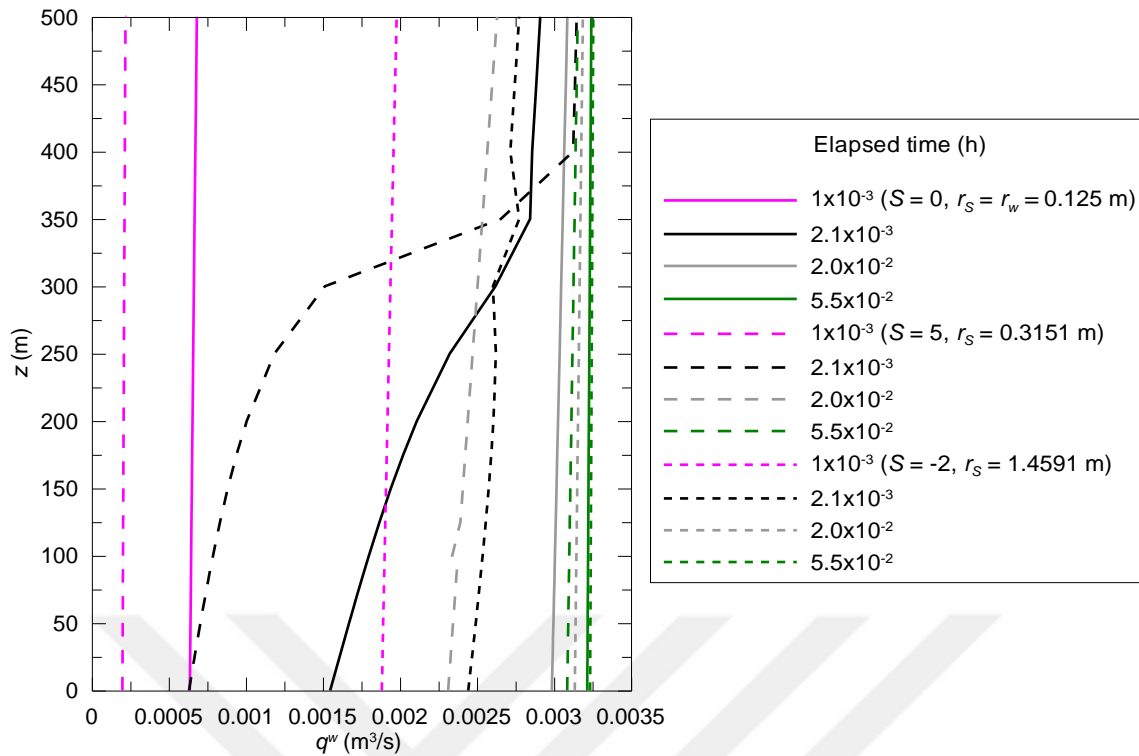


Figure 5.7:  $z$  vs  $dp^w/dz$  plot at various buildup elapsed times, momentum model, zero skin case.



**Figure 5.8:**  $z$  vs  $\text{abs}(dq^w/dz)$  plot at various buildup elapsed times, momentum model, zero skin case.



**Figure 5.9:** Effect of skin on  $q^w$  along the wellbore at various drawdown elapsed times, momentum model.

### 5.3 Wellbore Temperature Behavior for Production and Buildup Cases

Here, we observe the wellbore temperature behavior computed by analytical wellbore temperature solutions in the previous sections.

In Figure 13 and 14, we show the transient wellbore temperature distribution on a semilog plot for various different gauge locations with respect to drawdown and buildup time, respectively. These figures are obtained for zero skin case in the wellbore, with momentum effects. The wellbore temperature during drawdown and buildup is cooling due to heat loss to formation as the gauge location increases. The reason of heat loss to formations is the lower earth temperature at the gauge location, as shown in Figure 15 and 26. Because of the increased temperature of the fluid entering into the wellbore due to JT heating, the wellbore temperature at late times of drawdown at the gauge location increases. But, we can see that the wellbore temperature at late times of buildup tends to the earth temperature (constant) at the gauge location.

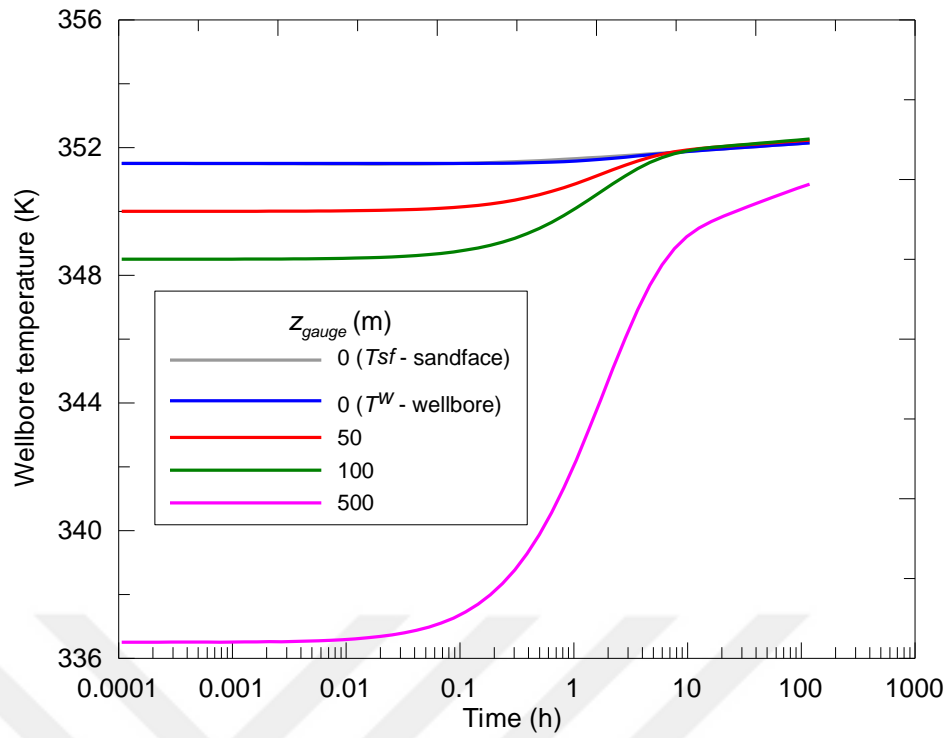


**Figure 5.10:** Effect of gauge location inside the wellbore on transient temperatures during drawdown; zero skin case.

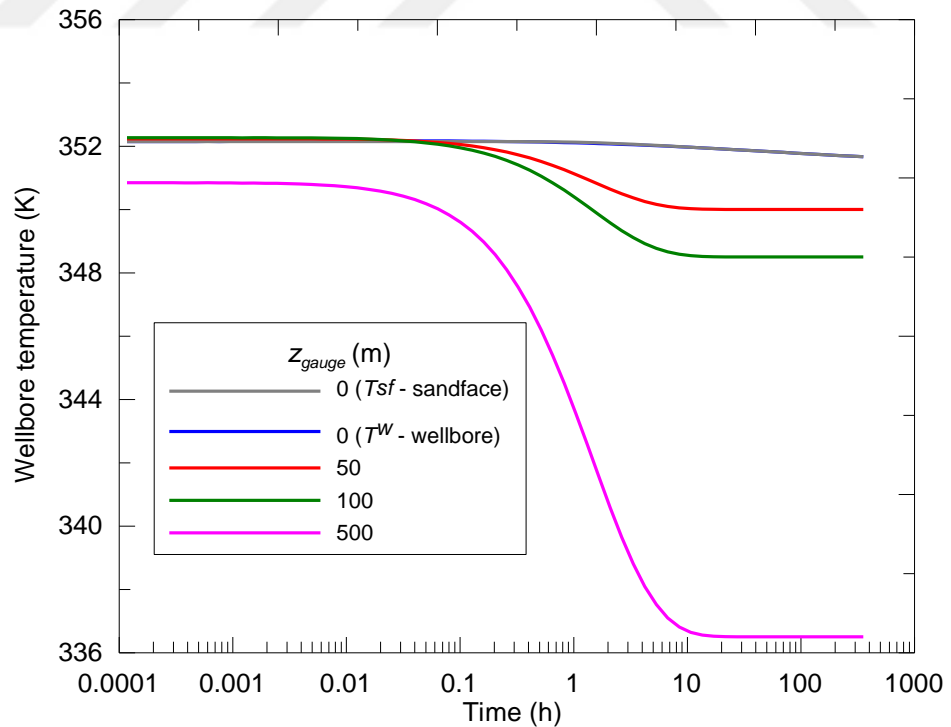


**Figure 5.11:** Effect of gauge location inside the wellbore on transient temperatures during buildup; zero skin case.

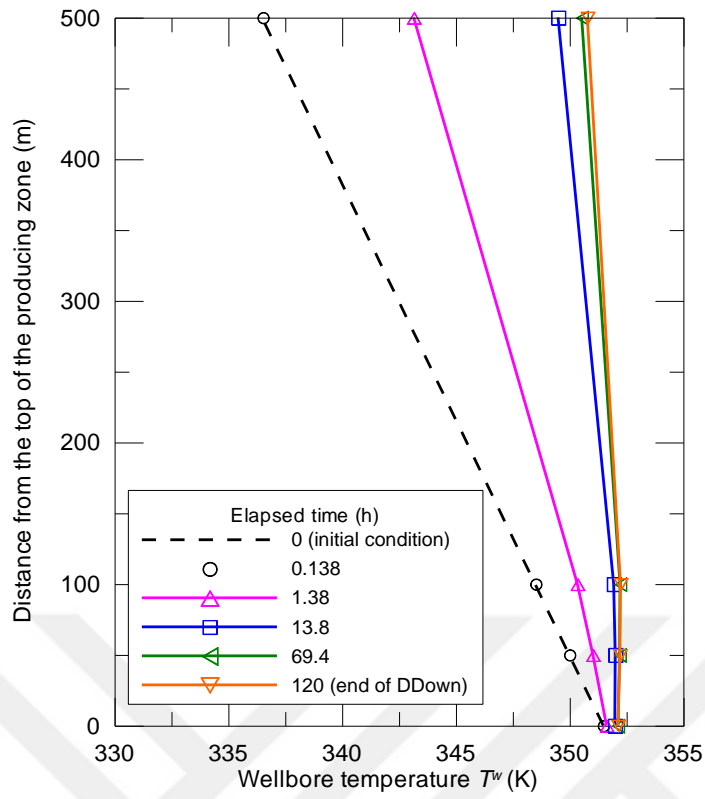


**Figure 5.12:**  $z$  vs  $T^w$  plot at various drawdown times, momentum model, zero skin case.

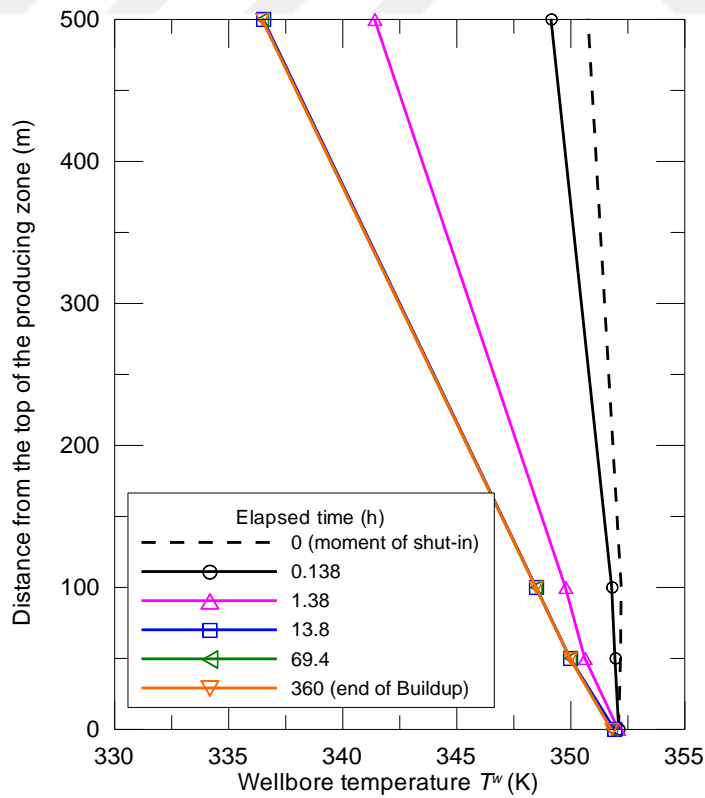


**Figure 5.13:**  $z$  vs  $T^w$  plot at various buildup times, momentum model, zero skin case.

## 6. IMPACT OF VARIOUS PARAMETERS ON SANDFACE AND WELLBORE TEMPERATURE

### 6.1 Geothermal Gradient at a Fixed Gauge Location for Production and Buildup

Here, we observe the effect of geothermal gradient for different skin cases in drawdown and buildup period. Our results are for fixed gauge location as  $z=500$  m. As shown in Figure 17, as the geothermal gradient increases, the wellbore temperature decreases in drawdown and buildup for all skin cases.

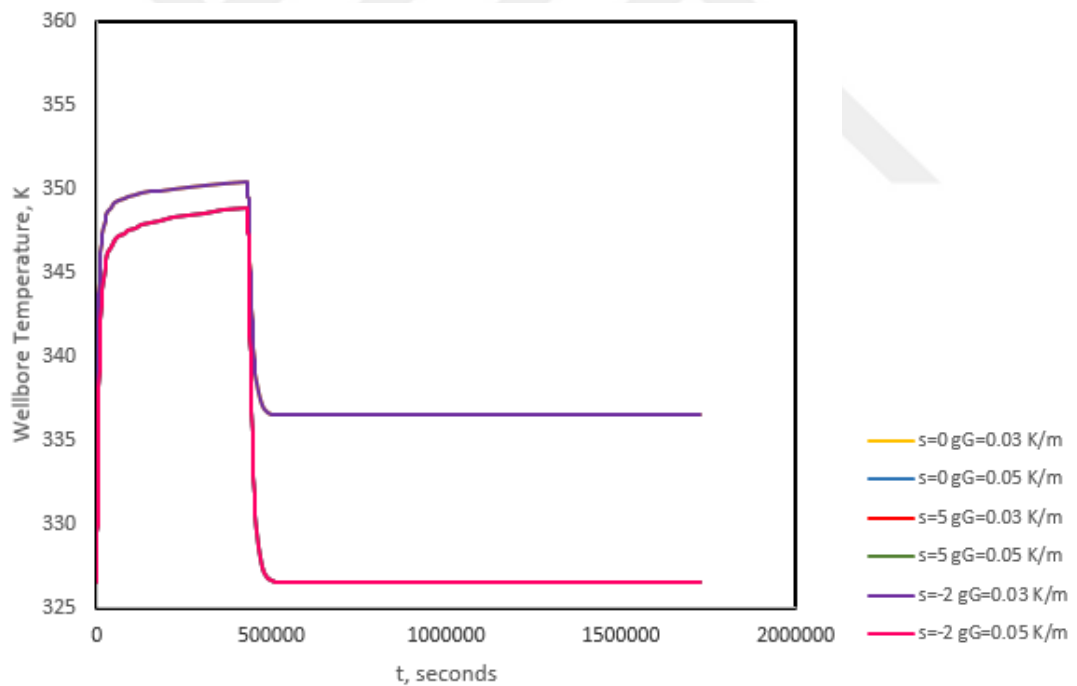


**Figure 6.1:** Effect of Earth Geothermal Gradient for  $z=500$  m

### 6.2 Effect of Earth Conductivity and Diffusivity at a Fixed Gauge Location in Production and Buildup

Here, we can see that the wellbore temperature decreases with increasing earth conductivity value for all skin cases in drawdown period, except early times. Earth conductivity does not have any effect in buildup period in Figure 18.

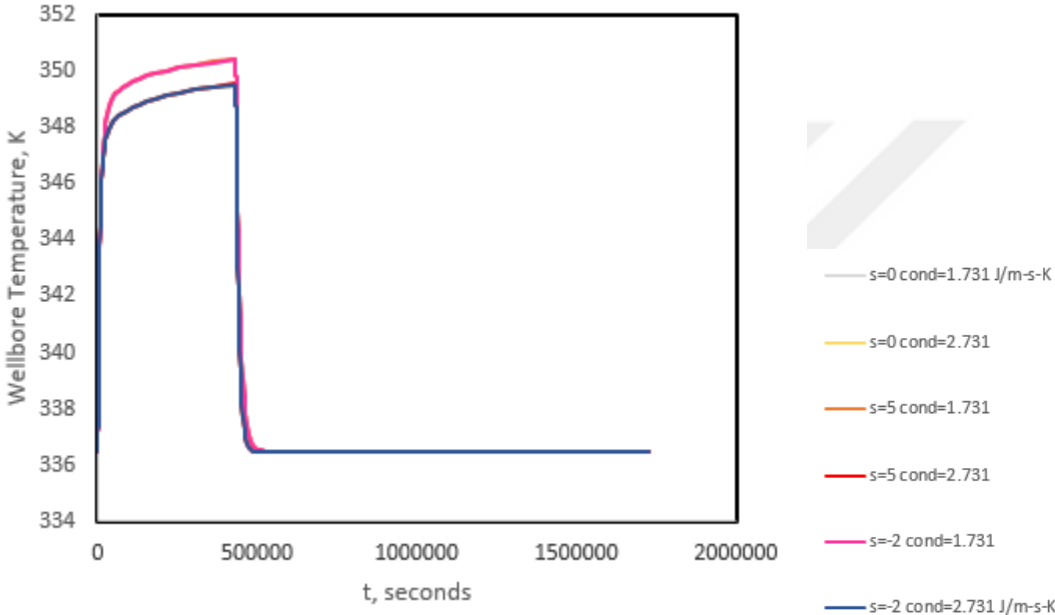
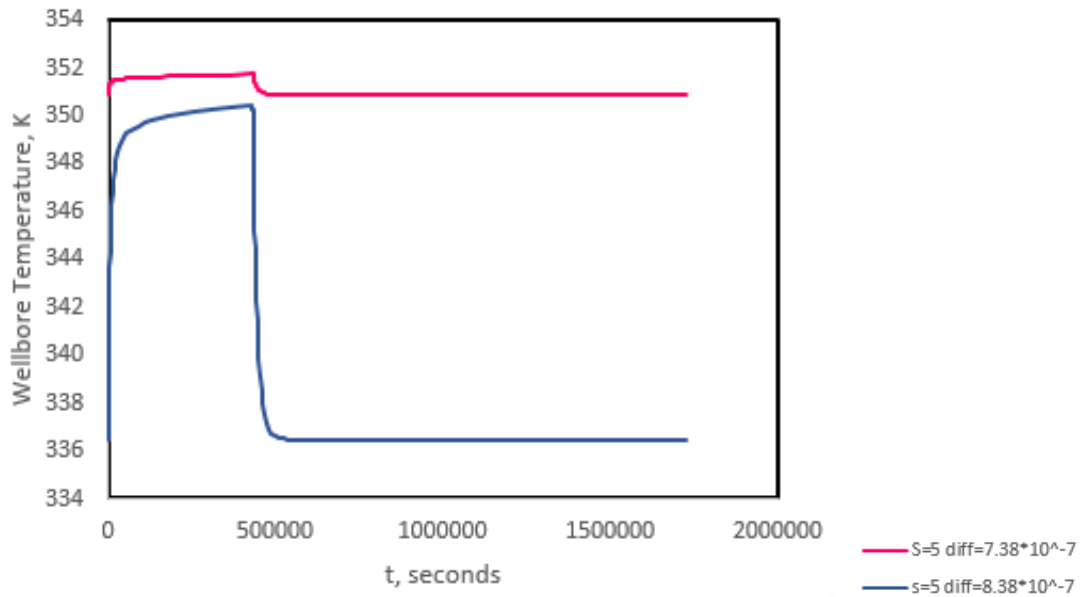


Figure 6.2: Effect of Earth Conductivity for z=500 m

As shown in Figure 24, we do not observe any vital effect of earth thermal diffusivity for zero and negative skin cases; however, a vital effect occurs for positive skin case in drawdown and buildup periods. For positive skin case, the wellbore temperature decreases significantly as earth thermal diffusivity decreases.



**Figure 6.3:** Effect of Earth Diffusivity for  $z=500$  m

### 6.3 Effect of Production Flow Rate at a Fixed Gauge Location

In this section, we observe the flow rate effects at a fixed gauge location. Two different gauge locations are evaluated for drawdown and buildup.

Firstly, three different flow rates are used as  $3.3 \times 10^{-4}$ ,  $3.3 \times 10^{-3}$  and  $3.3 \times 10^{-2}$  in  $z=0$  m gauge location with and without skin. As shown in Fig. 20, the wellbore temperature increases with increasing flow rate for  $s=0$  and  $s=5$  cases at  $z=0$  m gauge location.

Secondly, three different flow rates are used as  $3.3 \times 10^{-4}$ ,  $3.3 \times 10^{-3}$  and  $3.3 \times 10^{-2}$  in  $z=100$  m gauge location with and without skin. As shown in Figure 21, the wellbore temperature increases with increasing flow rate for  $s=0$  and  $s=5$  cases at  $z=100$  m gauge location, like in Figure 20. However, this increment of wellbore temperature at 100 m gauge location because of the flow rate is more distinct than at 0 m gauge location.

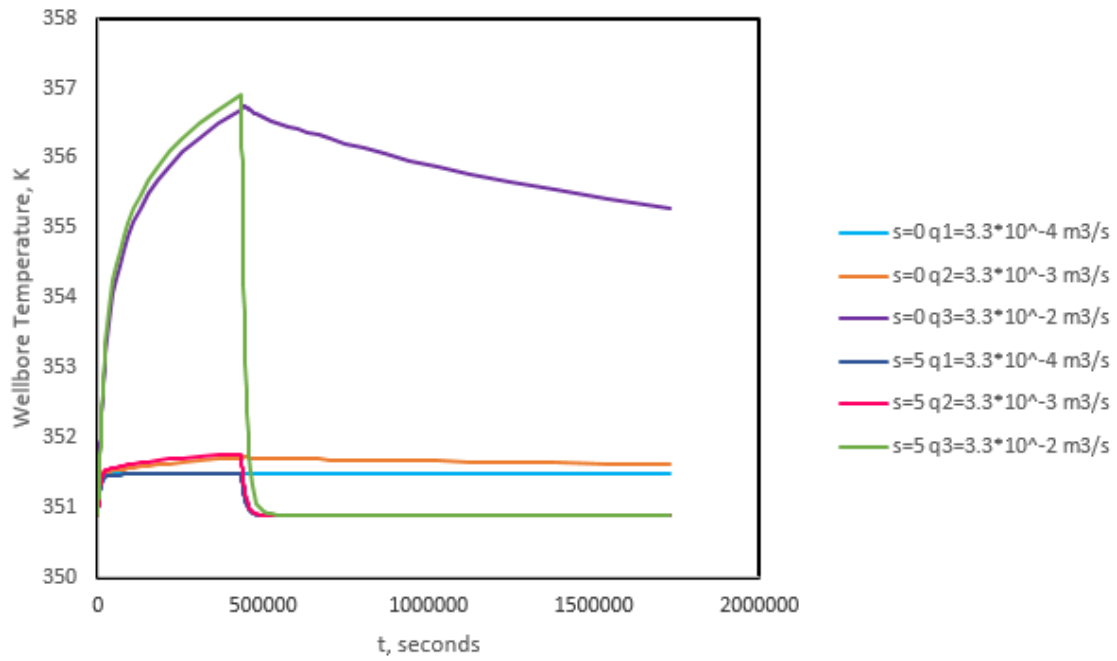


**Figure 6.4:** Effect of Production Flow Rate for  $z=0$  m

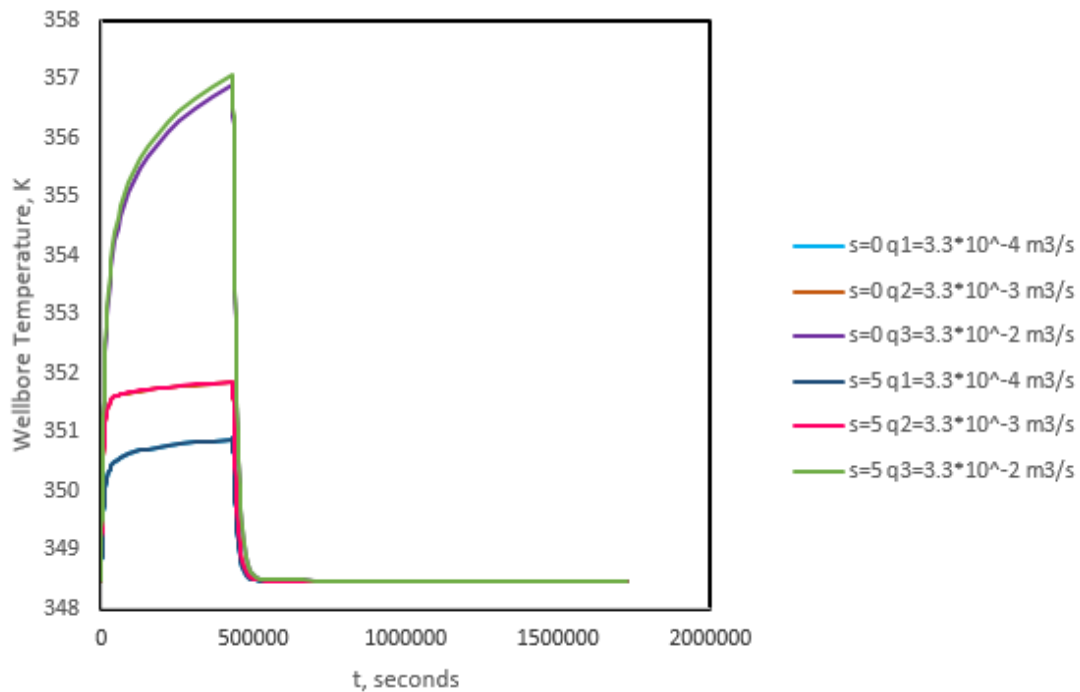


**Figure 6.5:** Effect of Production Flow Rate for  $z=100$  m

## 7. ANALYSIS OF INTERPRETATION OF TRANSIENT WELLBORE TEMPERATURES

We can see the comparison of sandface and wellbore drawdown and buildup temperature-derivatives with skin and momentum effects at different gauge locations in Figure 22 and 23, respectively. At early times, a unit-slope line can be seen in drawdown wellbore temperature-derivatives in Figure 22. As the gauge distance increases, the unit-slope line become longer. The late time derivatives show zero slope in drawdown reversing the non-skin zone properties. Also, we can see the intermediate-time zero slope reversing the skin zone properties. By defining flow regimes, we can estimate parameters such as permeability, skin, J-T coefficient, thermal conductivity of earth and formation from transient wellbore temperature solutions. As shown in Figure 23, we can not define any flow regimes for buildup wellbore temperature-derivatives.

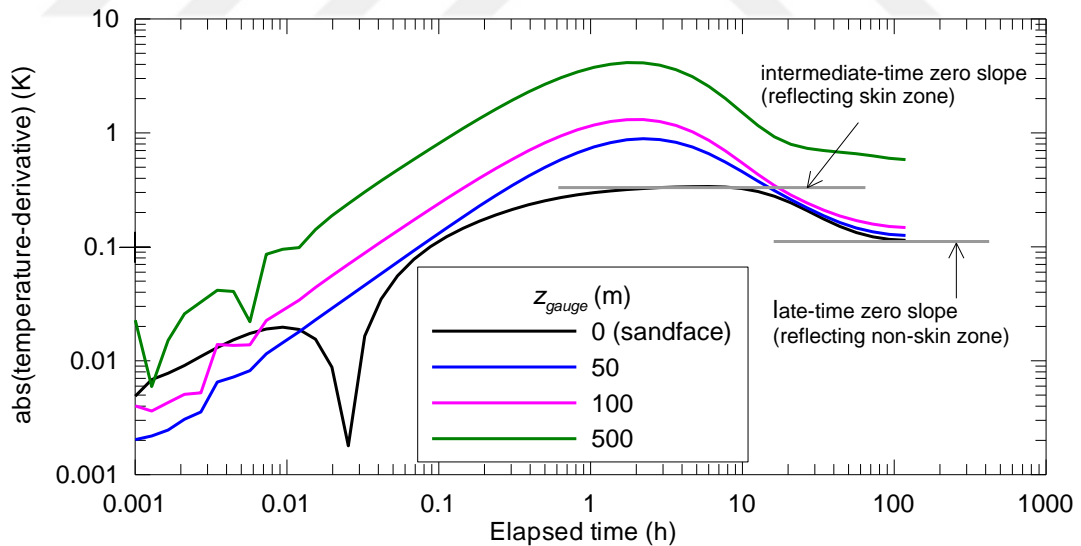


**Figure 7.1:** Comparison of sandface and wellbore drawdown temperature-derivatives with skin and momentum effects at different gauge locations (Onur et al.,2016)

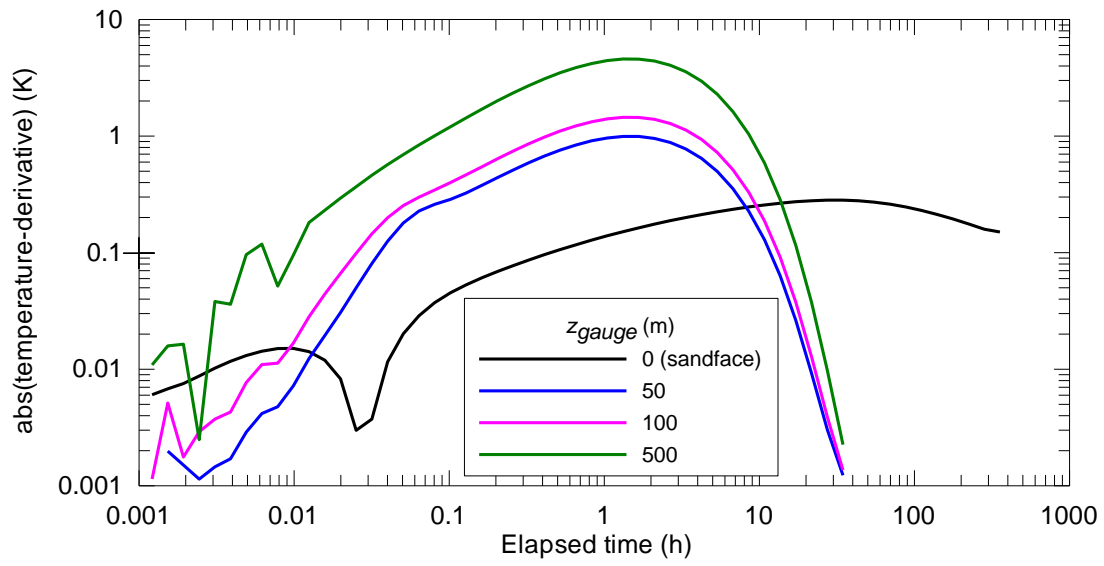


**Figure 7.2:** Comparison of sandface and wellbore buildup temperature-derivatives with skin and momentum effects at different gauge locations (Onur et al.,2016)

## 8. CONCLUSIONS

In this work, analytical nonisothermal wellbore model is presented to predict transient wellbore temperature data with momentum or wellbore storage effects. To obtain temperature behaviors for transient and steady state conditions in drawdown and buildup, we use conventional wellbore storage model, momentum model, and wellbore heat flow model equations. Also, this work provides analytical solutions by coupling with sandface/bottomhole pressure and temperature solutions. For coupling, we use the equations derived in Laplace space for variable-rate case including constant-rate and buildup periods by Kocak (2017). During this study, we assume slightly compressible and single-phase fluid in a homogeneous infinite-acting reservoir system, and reservoir system with skin modeled is a composite zone adjacent to the wellbore. In order to decouple the mass, momentum and energy balance equations in the wellbore and reservoir, we can ignore the impacts of temperature changes on wellbore and reservoir pressure transient data.

The analytical model is provided by using mass, momentum and wellbore heat flow model equations. Then, it is coupled with transient bottomhole and wellbore pressure solutions, and wellbore flow rate solutions derived by Kocak (2017) in Laplace space. With derived analytical model, we investigate the sandface and wellbore behaviors of flow rate, pressure, and temperature distributions. Besides, we investigate the impact of various parameters such as geothermal gradient, earth conductivity and diffusivity, production flow rate at a fixed gauge location on temperature distributions.

We can provide the conclusions obtained from the investigations:

- Unlike sandface temperature data, the wellbore temperature measurements above perforation zone may not show the early time and late time semilog straight lines reflecting the impacts of adiabatic-fluid and the J-T effects, respectively. Because, these semilog straight lines depend on length above perforation zone greatly. Also, they rely on earth geothermal gradient and radial heat losses.

- If the gauge location is near the producing zone, we can estimate the skin zone properties easily by using drawdown and buildup wellbore temperatures.
- The wellbore heat losses dominate in the buildup compared with drawdown; thus, the formation properties can not be predicted from buildup wellbore temperature.
- In drawdown, as the gauge location moves away from the producing zone, the wellbore heat losses dominate on the wellbore temperature data.
- We can not obtain any discernable flow regimes from buildup wellbore temperatures at gauge locations, unlike buildup sandface temperatures.



## REFERENCES

- Alves, I.N., Alhanati, F.J.S., & Shoham, O.** (1992). A Unified Model for Predicting Flowing Temperature Distribution in Wellbores and Pipelines. *SPE Prod Eng* **7** (4): 363-367. SPE-20632-PA. <https://doi.org/10.2118/114705-PA>.
- App, J.F.** (2009). Nonisothermal and Productivity Behavior of High-Pressure Reservoirs, SPE 114705-MS, presented SPE Annual Technical Conference, Denver. <https://doi.org/10.2118/114705-MS>.
- Crump, K.S.** (1976). Numerical Inversion of Laplace Transforms Using a Fourier Series Approximation. *J Assoc Comput Mach* **23** (1): 89-96. <http://dx.doi.org/10.1145/321921.321931>.
- Duru, O.O. & Horne, R.N.** (2010). Modeling Reservoir Temperature Transients and Reservoir-Parameter Estimation Constrained to the Model, SPE-115791-PA, presented SPE Annual Technical Conference, Denver. <https://doi.org/10.2118/115791-PA>
- Hasan, A.R., Lin, D. & Kabir, C.S.** (2005). Analytical Wellbore-Temperature Model for Transient Gas-Well Testing, SPE-84288-PA. <https://doi.org/10.2118/84288-PA>.
- Izgec, B., Kabir, C.S., Zhu, D., & Hasan, A.R.** (2007). Transient Fluid and Heat Flow Modeling in Coupled Wellbore/Reservoir Systems, SPE-102070-MS, presented SPE Annual Technical Conference, San Antonio, Texas. <https://doi.org/10.2118/102070-MS>.
- Kocak, S.** (2017). *Modeling and Interpreting Transient Sandface Temperatures in Presence of Momentum and Skin Effect Under Nonisothermal Single-Phase Liquid Flow Conditions in Oil Reservoirs*. MS Thesis, Dep. Of Pet. and Nat. Gas Eng., ITU Graduate School of Science Engineering and Technology, Istanbul Technical University, Istanbul, Turkey.
- Onur, M. & Cinar, M.** (2016). Temperature Transient Analysis of Slightly Compressible, Single Phase Reservoirs. Presented at the SPE Europec featured at 78<sup>th</sup>EAGE Conference and Exhibition, Vienna, Austria, 30

May-2

June.

SPE-180074-MS.

<https://doi.org/10.2118/180074-PA>.

**Onur, M., Ulker, G., Kocak, S., & Gok, I. M.** (2016). Interpretation and Analysis of Transient Sandface and Wellbore Temperature Data. Society of Petroleum Engineers. <https://doi.org/10.2118/181710-MS>.

**Palabiyik, Y., Tureyen, O.I., and Onur, M.** (2013). A Study on Pressure and Temperature Behaviors of Geothermal Wells in Single-Phase Liquid Reservoirs. Oral presentation given at the 38<sup>th</sup> Workshop on Geothermal Reservoir Engineering, Stanford University, Stanford, California, 11-13 February.

**Palabiyik, Y., Tureyen, O.I., and Onur, M.** (2015). Pressure and Temperature Behaviors of Single-Phase Liquid Water Geothermal Reservoirs under Various Production/Injection Schemes. Oral presentation given at the World Geothermal Congress, Melbourne, Australia, 19-25 April.

**Ramey, H. J. Jr.** (1962). Wellbore Heat Transmission. *J Pet Technol* 14 (4): 427-435. SPE-96-PA. <https://doi.org/10.2118/96-PA>.

**Sagar, R., Doty, D.R., and Schmidt, Z.** (1991). Predicting Temperature Profiles in a Flowing Well. *SPE Prod Eng* 6 (4): 441-448. SPE-19702-PA. <https://doi.org/10.2118/19702-PA>.

**Sidorova, M., Shako V., Pimenov V. et al.** (2015). The value of transient temperature responses in testing operations. Presented at the SPE Middle East Oil & Gas Show and Conference, Manama, Bahrain, 8-11 March. SPE-172758-MS. <http://dx.doi.org/10.2118/172758-MS>.

**Stehfest, H.** (1970). Algorithm 368: Numerical Inversion of Laplace Transforms. *Comm. ACM* 13 (1): 47-49. <http://dx.doi.org/10.1145/361953.361969>.

**Sui, W., Zhu, D., Hill, A.D. et al.** (2008a). Model for Transient Temperature and Pressure Behavior in Commingled Vertical Wells. Presented at the SPE Russian Oil and Gas Technical Conference and Exhibition, Moscow, 28-30 October. SPE-115200-MS. <https://doi.org/10.2118/115200-ms>.

**Sui, W., Zhu, D., Hill, A.D. et al.** (2008b). Determining Multilayer Formation Properties from Transient Temperature and Pressure Measurements.

Presented at the SPE Annual Technical Conference and Exhibition,  
Denver, 21-24 September. SPE-116270-MS.  
<https://doi.org/10.2118/116270-MS>.





## CURRICULUM VITAE



**Name Surname** : Gonca ÜLKER

**Place and Date of Birth** : MECİTÖZÜ 16.06.1992

**E-Mail** : ulker@itu.edu.tr

### EDUCATION

- **B.Sc.** : 2015, Istanbul Technical University, Faculty of Mines, Petroleum and Natural Gas Engineering

### PUBLICATIONS, PRESENTATIONS AND PATENTS ON THE THESIS:

- Onur, M., Ulker, G., Kocak, S., & Gok, I. M. (2016, September 26). Interpretation and Analysis of Transient Sandface and Wellbore Temperature Sata. Society of Petroleum Engineers. doi:10.2118/181710-MS